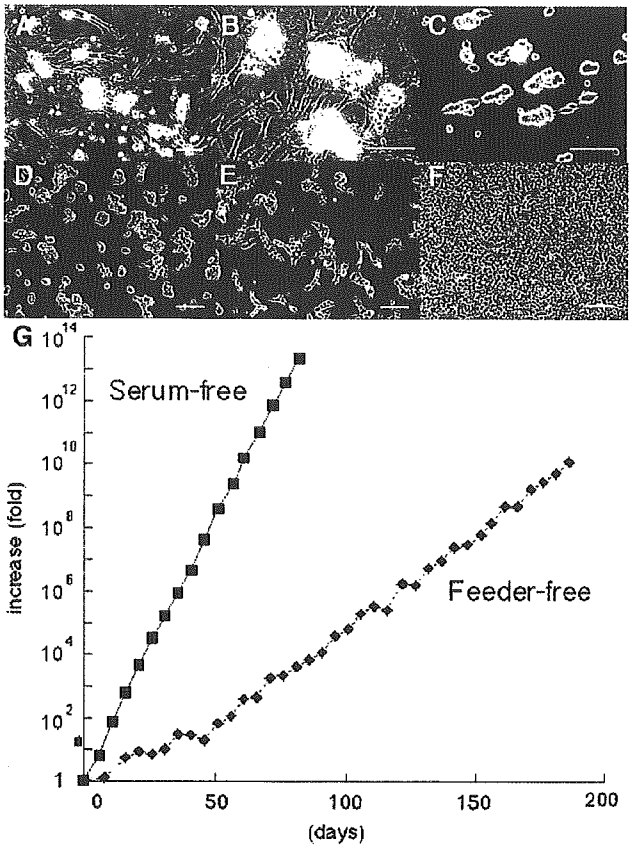

FIG. 1. In vitro growth of GS cells. A) Fully established GS cells on MEFs in serum-containing medium. B) GS cells on MEFs in serum-free medium. C–F) GS cells on laminin: (C) clump-type colonies that resemble GS cells on MEFs, (D) colonies are round; (E) chain formation of GS cells on laminin, (F) confluent GS cells in the culture well. G) Proliferation of GS cells in serum-free or feeder-free conditions. Bar = 100 μm.

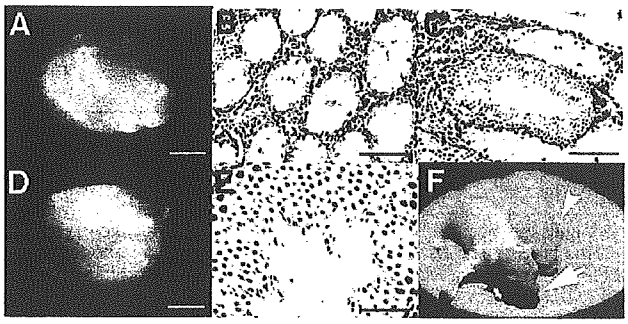

FIG. 3. Spermatogenesis and offspring production from cultured cells. A) A recipient testis that received EGFP-expressing donor GS cells from serum-free culture. B) Histological appearance of W mouse testis (untransplanted control). Note the absence of differentiated germ cells. C) Histological appearance of a W mouse testis that received donor GS cells from the serum-free culture. Note the normal-appearing spermatogenesis and elongated spermatids. D) A recipient testis that received GFP-expressing donor GS cells from the feeder-free culture. E) Histological appearance of the recipient testis showing normal spermatogenesis. F) F2 offspring that resulted from GS cells from feeder-free culture. The presence of the donor transgene is evidenced by the green fluorescence under UV light (arrow). No fluorescence was observed in the control litter (arrowhead). Bar = 1 mm (A and D), 100 μm (B and C), 50 μm (E).

5-fold after 5 days in medium containing 1% serum, they expanded up to 12-fold in the serum-free culture over the same culture period. Flow cytometric analysis showed no significant changes in cell surface marker expression owing to the removal of serum: GS cells strongly expressed EpCAM [33], CD9 [34], and α6- and β1-integrin [20]; the cells weakly expressed c-kit [35] and did not express SSEA-1 [36] (Fig. 2A). RT-PCR analysis showed that the cultured cells also expressed other primordial germ cell (PGCs) or spermatogonia markers, including Oct-4 [37] (Fig. 2B).

To examine whether the cultured cells have the ability to colonize seminiferous tubules, we used a spermatogonial transplantation technique [38]. This technique allows competent spermatogonial stem cells to recolonize the empty seminiferous tubules of infertile animals and to differentiate into mature spermatozoa. EGFP-expressing GS that had been cultured for 6 to 52 days in serum-free culture were transplanted into the seminiferous tubules of immune-suppressed W mice [28] (Fig. 3A). W animals lack differentiating germ cells as a result of mutations in the *c-kit* gene [39] (Fig. 3B); therefore, any spermatogenesis in the recipient testis is derived from cultured donor cells. After different numbers of passages, the cells were transplanted

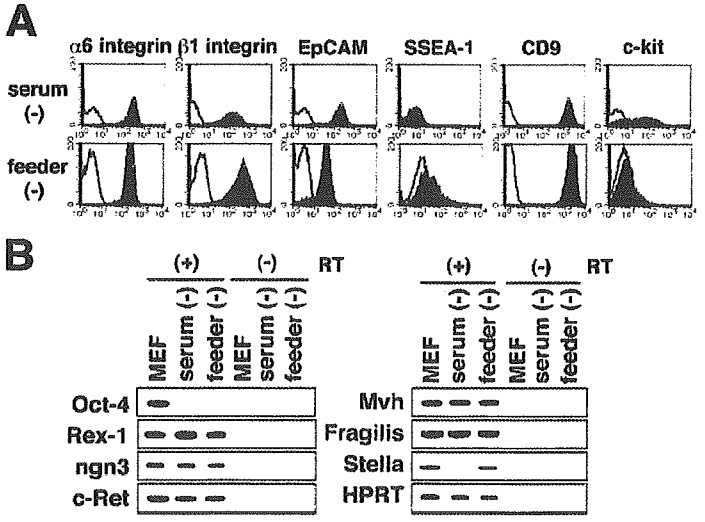

FIG. 2. Phenotypic characterization of cultured cells. A) Flow cytometric characterization. GS cells were stained with antibodies against α6-integrin, β1-integrin, EpCAM, SSEA1, CD9, and c-kit. Only EGFP-positive cells were gated to analyze GS cells in the serum-free culture. B) RT-PCR analysis. Specific primers were used to amplify cDNA from GS cells under serum-free or feeder-free culture conditions.

TABLE 1. Spermatogonial stem cell expansion in serum-free culture.[a]

Days to transplant[b] (passage)	GS cells injected/testis ($\times 10^4$)	Colonies/testis	Colonies/10^5 GS cells	Stem cells/10^5 GS cells[c]	Increase in GS cell number[d,e] (fold)	Increase in stem cell number[d,f] (fold)
6 (1)	1.5	20.0 ± 6.9	133.3 ± 46.0	1333		
11 (2)	1.5	9.9 ± 2.9	65.7 ± 19.6	657	12.1	6.0
16 (3)	1.5	19.2 ± 3.7	128.0 ± 24.7	1280	103.3	99.2
52 (10)	1.5	15.2 ± 0.6	101.3 ± 3.9	1013	8.5×10^7	6.5×10^7

[a] Values are mean ± SEM. Results from at least four recipient testes for each transplantation.
[b] The number of days from initiation of serum-free culture to transplantation.
[c] It is assumed that 10% of transplanted stem cells can colonize the testis [29].
[d] The increase in GS or stem cell number from the first transplantation.
[e] (Total GS cell number at indicated time point)/(cell number at Day 6).
[f] (Increase in GS cell number at indicated time point; column 6) × (stem cells/10^5 GS cells at indicated time point; column 5)/(stem cells/10^5 GS cells at Day 6; column 5, row 2). For example, at 52 days, $(8.5 \times 10^7) \times 1013/1333 = 6.5 \times 10^7$.

again to measure the increase in stem cell number during this period. Two months after transplantation, the recipient mice were killed, and colonies in the testes were counted under UV light illumination.

As shown in Table 1, approximately 6.5×10^7-fold expansion of stem cell number was observed during 46 days in culture, during which the total cell number increased 8.5×10^7-fold (Fig. 1G). Assuming 10% colonization efficiency of stem cells [29], the concentrations of stem cells in culture ranged from 0.66% to 1.33%. Histological analysis of the recipient testis confirmed the presence of normal-appearing spermatogenesis (Fig. 3C). Mature spermatogenic cells were observed in the seminiferous tubules. The cells continued to grow in serum-free conditions for at least 3 mo. These results indicate that GS cells can expand in serum-free conditions and that they have the ability to undergo normal spermatogenesis when transferred into the seminiferous tubule environment.

Feeder-Free Culture of Mouse GS Cells

We then investigated the role of feeder cells in GS cell expansion. We previously showed that freshly prepared spermatogonial stem cells attach preferentially to laminin [20]; the stem cell concentration could be enriched 3- to 8-fold after selection on a laminin-coated plate [40, 41]. Based on this observation, we hypothesized that laminin would replace MEFs in supporting GS cell growth. To test this possibility, EGFP-expressing GS cells that had been cultured on MEFs for 60 days were transferred onto laminin.

In this experiment, we examined various combinations of cytokines and also tested the effect of conditioned medium from MEFs in some experiments, because it is essential for human ES cells to remain undifferentiated under feeder-free culture conditions [19]. As shown in Table 2, GS cells were able to proliferate under all five conditions tested. The cells continued to grow as long as the medium contained GDNF, and either EGF or bFGF was sufficient to promote GS cell growth in medium containing 1% FCS. However, cells could not grow in the absence of GDNF, even when the medium was supplemented with both EGF and bFGF. Only after GDNF supplementation did cells resume proliferation. We did not find statistical differences in the proliferation rate between treatment groups. The presence of serum was essential for the success of feeder-free culture, as GS cells did not attach to laminin when cultured in the serum-free medium.

Upon transfer to laminin, GS cells gradually changed their morphology. While GS cells generally formed clumps on MEFs (Fig. 1A), they formed various patterns on lam-

TABLE 2. Spermatogonial stem cell expansion in feeder-free culture.[a]

Experiment	Growth factor[b]	Days to transplant[c] (passage)	GS cells injected/testis ($\times 10^4$)	Colonies/testis	Colonies/10^5 GS cells	Stem cells/10^5 GS cells[d]	Increase in GS cell number (fold)[e]	Increase in stem cell number (fold)[e,i]
1	E + F + G + L + CM	31 (5)	5.4	41.2 ± 5.7	76.1 ± 10.6	761		
		56 (10)	7.2	22.7 ± 4.5	31.8 ± 6.3	318	11.5	4.8
		91 (17)	4.6	52.3 ± 6.4	111.8 ± 1.4	1118	1.19×10^3	1.7×10^3
		186 (36)	1.5	15.0 ± 4.4	100.0 ± 30.0	1000	1.24×10^9	1.6×10^9
2	E + F + G + CM	20 (4)	4.8	21.2 ± 6.0	44.7 ± 12.6	447		
		106 (22)	1.5	17.5 ± 7.7	116.2 ± 52.1	1162	3.2×10^5	8.3×10^5
3	E + F + G	15 (3)	16.4	51.8 ± 3.4	31.4 ± 2.0	314		
		35 (7)	3.8	12.0 ± 3.1	31.4 ± 7.9	314	33.4	33.4
4	E + F + G	9 (2)	19.0	19.2 ± 5.5	10.1 ± 2.9	101		
		34 (7)	3.5	1.5 ± 1.2	4.3 ± 3.5	43	7.0	3.0
5	E + G	11 (2)	1.8	22.3 ± 13.4	126.3 ± 76.8	1263		
		50 (10)	11.3	17.2 ± 2.3	15.1 ± 1.9	151	206.8	24.7
6	F + G	39 (8)	10.1	12.2 ± 2.0	12.1 ± 2.0	121		
		59 (12)	1.4	2.8 ± 0.6	19.2 ± 4.3	192	17.7	28.1

[a] Values are mean ± SEM. Results are at least four recipient testes.
[b] E, EGF; F, bFGF; G, GDNF; L, LIF; CM, conditioned medium.
[c] The number of days from initiation of feeder-free culture to transplantation.
[d] It is assumed that 10% of transplanted stem cells can colonize the testis [29].
[e] The increase in GS or stem cell number from the first transplantation.
[i] (Increase in GS cell number at indicated time point) × (stem cells/10^5 GS cells at indicated time point)/(stem cells/10^5 GS cells at first transplantation).

inin, including clumps (Fig. 1C), and had a fibroblast-like appearance (Fig. 1D). Occasionally, cells formed chains or networks (Fig. 1E), which resembled the proliferative patterns of spermatogonial stem cells observed in vivo after spermatogonial transplantation [29]. The morphology of cells in feeder-free culture appeared to depend on the cell density, and no particular cytokine combination or MEF-conditioned medium influenced the proliferative patterns. Generally, cells tended to form clumps at low cell density, but they became fibroblastic at high cell density. When seeded at relatively high density, GS cells proliferated and spread on the bottom of the well, and GS cells covered the entire surface of the well (Fig. 1F).

To confirm the phenotype, the cultured cells were analyzed using flow cytometry for the expression of cell surface markers (Fig. 2A). The cells on laminin had a similar phenotype to GS cells on MEFs; however, not only was the expression of c-kit reduced, but the expression of SSEA-1 was initiated. Whereas GS cells on MEFs do not express SSEA-1 [11], a significant proportion of the cells on laminin expressed this molecule. No significant difference was noted in the cell surface marker expression regardless of the type of cytokine (data not shown). RT-PCR analysis showed that the cultured cells not only expressed PGC markers (Fragilis, Stella) but also a spermatogonia marker (ngn3) [24, 42] (Fig. 2B). As SSEA-1 is expressed on PGCs, but not on spermatogonia [43], this suggested that the feeder-free culture changed the cell surface marker expression and induced a partial embryonic phenotype.

To examine whether the cultured cells still retain the ability to colonize seminiferous tubules and produce spermatogenesis, EGFP-expressing GS cells that had been cultured for different periods (ranging from 9 to 39 days) were recovered using trypsin and were microinjected into the seminiferous tubules of immune-suppressed W mice (Fig. 3D). After 4 to 31 passages, the cells were collected again at 35 to 186 days to measure the increase in stem cell numbers during this period. At least two different cultures with the same cytokine combinations were transplanted. The analysis of colony numbers in the recipient testis indicated that stem cell number increased in all five experiments regardless of the cytokine combination. Assuming 10% colonization efficiency of stem cells [29], the concentration of stem cells ranged from 0.04% to 1.26%. The total cell number increased approximately 1.2×10^9-fold during the 6-mo culture period (Fig. 1G). Statistical analyses revealed that colonization of GS cells was most efficient when GS cells were cultured in culture supernatant of MEFs ($P < 0.05$ by t-test). LIF was also beneficial for colonization ($P < 0.05$ by t-test), but we did not find significant difference between EGF and bFGF. Histological sections confirmed the presence of spermatogenesis in the recipient testis, and all stages of spermatogenic cells were found (Fig. 3E).

To further confirm that these germ cells are functionally normal, we attempted to derive offspring from the cultured cells using microinsemination, a technique commonly used to derive offspring from infertile animals and humans [30, 44]. EGFP-expressing GS cells were cultured for 4 mo in feeder-free condition, and transplanted into three immune-suppressed W mice. Approximately 1.5×10^4 cells were microinjected into each testis. Four months after transplantation, two of the recipients were killed because they remained infertile after transplantation. Their testes were dissociated mechanically, and live spermatogenic cells were recovered by repeated pipetting of colonized tubule fragments; EGFP expression was identified under UV light. The cell suspension was kept frozen and stored in liquid nitrogen. After storage for 21 days, mature spermatozoa or elongated spermatids were microinjected into oocytes derived from C57BL/6 × DBA/2 F1 mice. A total of 83 eggs were constructed, and 56 eggs that developed to the two-cell stage were transferred to five pseudopregnant female recipients the day after microinsemination. The recipient females sired a total of 11 offspring, and 9 of them grew into adults: 4 males and 5 females. These offspring were fertile and could transmit the EGFP gene to the next generation (Fig. 3F). Therefore, these results indicate that GS cells in feeder-free culture retain the ability to colonize seminiferous tubules and can differentiate normally to produce fertile offspring.

TABLE 3. Frequency of spermatogonial stem cells in various conditions.

Condition	Colonies/10^5 cells	Reference
Wild-type	2.5	[29]
Cryptorchid	18.6	[45]
Sorted[a]	282.6	[45]
Serum (+), feeder (+)	12.1	[11]
Serum (−), feeder (+)	107.1	This study
Serum (+), feeder (−)[b]	79.9	This study

[a] β2 microglobulin⁻ Thy-1⁺ cells from cryptorchid testis.
[b] Results from E + F + G + L + CM in Table 2.

DISCUSSION

In this study, we showed that spermatogonial stem cells can expand in the complete absence of serum or somatic feeder cells in vitro. We used serum in our previous experiments [11], because adding serum was necessary to induce the initial development of GS cells from neonatal gonocytes. Although several attempts have been made to culture spermatogonial stem cells under serum-free conditions [45–47], it has been impossible to induce long-term proliferation of spermatogonial stem cells. In this study, we found that the initiation and maintenance of GS cell culture appear to be distinct processes, and that the maintenance of fully established GS cell does not require serum. Given that GS cell culture starts from gonocytes in the neonatal stage and that established GS cells have spermatogonia characteristics [11], gonocytes seem to acquire the characteristics of spermatogonia during in vitro culture, and some components in serum are required for this conversion. The development of spermatogonia from gonocytes probably involves multiple differentiation steps, reflected in the changes in morphology or cell surface markers of stem cells [48–50]. A recent study also showed that prepubertal germ cells are twice as viable in vitro [47]. Therefore, it is not surprising that the two cell types have different growth requirements. Although further studies are required to determine the factors that influence the conversion of gonocytes into spermatogonia or GS cells, the serum-free culture of established GS cells will be useful for characterizing the mechanisms regulating the proliferation and differentiation of spermatogonial stem cells.

Stem cells usually require stromal cells to maintain their undifferentiated state both in vivo and in vitro [10, 14, 15, 51]. In spermatogonial stem cell culture, it was initially reported that mouse spermatogonial stem cells could survive in vitro for approximately 4 mo on STO feeder, but they disappear within 1 wk when they are cultured directly on a tissue culture dish [52], which suggested that the feeder layer is essential for maintaining spermatogonial stem cells in vitro. However, subsequent studies revealed that the

number of spermatogonial stem cells decreased in culture even on STO feeder, and only 10% to 20% of the stem cells could be recovered after 1 wk in vitro [53]. Similar results were recently reported in rats [54, 55]. The type of feeder cells affected stem cell survival; rat spermatogonial stem cells survived longer on Sertoli cells than they did on STO cells [55], but another study showed that Sertoli cells had a negative effect on spermatogonial stem cells in mice [53]. While these culture conditions failed to induce long-term proliferation of spermatogonial stem cells, our results demonstrate that laminin can substitute for the MEFs, indicating that a feeder layer is not essential for inducing the self-renewal division of spermatogonial stem cells [2].

Of interest, several differences were noted between the feeder-free culture condition and MEF-based culture. For example, GS cells on laminin tend to form various types of colonies, ranging from chains to clumps, whereas those on MEFs generally form clumps. The formation of chain-type colonies was reminiscent of spermatogenic colonies after spermatogonial transplantation into a seminiferous tubule environment [29]. Conversely, the formation of clump-type colonies was also observed in vivo, when GDNF was overexpressed in Sertoli cells [56]. GDNF is an essential factor for the self-renewing division of spermatogonial stem cells [57]; the overexpression of GDNF resulted in the loss of differentiation of germ cells and induced clump formation and expansion of spermatogonial stem cells in vivo [56]. These observations suggested that colony morphology is dependent on the amount of GDNF and that spermatogonial stem cells normally proliferate with chain formation, forming clumps when the proliferation of stem cells is strongly stimulated. In our study, because GDNF was used at the same concentration throughout the experiments, the result suggest that MEFs enhance the effect of GDNF, or exert a positive effect by secreting some other molecules that stimulate the proliferation of spermatogonial stem cells. This is supported by our observation that the GS cell growth on laminin was slower than that using MEFs. Thus, the cell-cell interaction between stem cells and MEFs may provide an additional growth stimulus, which was manifested as the changes in the colony morphology.

Another unexpected feature of the feeder-free culture was the changes in surface marker expression. In particular, the expression of SSEA-1 was unexpected. SSEA-1 is expressed on early embryos and PGCs, but its expression disappears after midgestation [43]. Conversely, GS cells on laminin also expressed ngn3, which is a marker of undifferentiated spermatogonia in the postnatal testis [24]. The ratio of cells expressing c-kit was also reduced in the feeder-free culture. Therefore, the pattern of gene expression in GS cells is influenced by the culture environment. Currently, we do not know why GS cells start to express such an embryonic marker in feeder-free culture. Although we cannot exclude the possibility that this reflects the abnormal reaction of spermatogonial stem cells to the unphysiological environment, it is possible that there is a rare population of spermatogonial stem cells that express SSEA-1 in vivo. Because there are very few stem cells (only 2 to 3 cells in 10^4 testis cells) [2, 58], it is possible that such a rare population escapes detection using conventional immunohistological methods on testis sections. Alternatively, perhaps GS cells have the potential to change into cells with more primitive characteristics.

Despite the different colony morphology and surface marker expression, GS cells on laminin retained the capacity to produce spermatogenic colonies and offspring following transplantation into infertile mice. Given the ability to self-renew as the defining characteristics of stem cells, these results indicate that cultured cells have stem cell activity as spermatogonial stem cells. Although the expression of SSEA-1 suggested a fetal phenotype of GS cells, spermatogenesis occurred efficiently in transplant recipients, which indicates that GS cells on laminin are functionally comparable to spermatogonial stem cells. Although direct comparison was not made, the frequency of stem cells in feeder-free culture was significantly higher than that reported in our previous study using MEFs (Table 3). Because it is possible to collect a large number of stem cells from culture, it provides a new approach for characterizing stem cells. For example, it may be easier to obtain a more pure population of stem cells from culture than currently achieved using primary cells from cryptorchid testis. Combined, our findings demonstrate that direct contact with somatic stromal cells is not necessary for the self-renewal division of spermatogonial stem cells and that cytokines and laminin can replace at least some aspects of niche function.

While this study provides the first step in reproducing the self-renewal division of spermatogonial stem cells under defined condition in vitro, an improved culture system is clearly necessary to allow more detailed analysis of self-renewal division and its relationship with its niche. Although laminin was able to replace MEFs in the serum-containing culture, it was not possible to culture GS cells on laminin under serum-free condition. It will also be important to establish culture conditions that direct a specific type of self-renewal, such as asymmetric division or self-renewing division [2]. In this sense, our results will be useful because serum-free and feeder-free culture systems will allow more definitive experiments to test the effect of individual factors on stem cells. The identification of critical factors will increase our knowledge of how the self-renewal division of spermatogonial stem cells is regulated and will lead us to develop more efficient techniques for male germline modification.

ACKNOWLEDGMENT

We thank Ms. A. Wada for her technical assistance.

REFERENCES

1. de Rooij DG, Russell LD. All you wanted to know about spermatogonia but were afraid to ask. J Androl 2000; 21:776–798.
2. Meistrich ML, van Beek MEAB. Spermatogonial stem cells. In: Desjardins C, Ewing LL (eds.), Cell and Molecular Biology of the Testis. New York: Oxford University Press; 1993:266–295.
3. Chiarini-Garcia H, Raymer AM, Russell LD. Non-random distribution of spermatogonia in rats: evidence of niches in the seminiferous tubules. Reproduction 2003; 126:669–680.
4. Schöfield R. The relationship between the spleen colony-forming cell and the heamopoietic stem cells. Blood Cells 1978; 4:7–25.
5. Kiger AA, White-Cooper H, Fuller MT. Somatic support cells restrict germline stem cell self-renewal and promote differentiation. Nature 2000; 407:750–754.
6. Tran J, Brenner TJ, DiNardo S. Somatic control over the germline stem cell lineage during *Drosophila* spermatogenesis. Nature 2000; 407:754–757.
7. Yamashita YM, Jones DL, Fuller MT. Orientation of asymmetric stem cell division by the APC tumor suppressor and centrosome. Science 2003; 301:1547–1550.
8. Kiger AA, Jones DL, Schulz C, Rogers MB, Fuller MT. Stem cell self-renewal specified by JAK-STAT activation in response to a support cell cue. Science 2001; 294:2542–2545.
9. Tulina N, Matunis E. Control of stem cell self-renewal in *Drosophila*

spermatogenesis by JAK-STAT signaling. Science 2001; 294:2546–2549.
10. Spradling A, Drummond-Barbosa D, Kai T. Stem cells find their niche. Nature 2001; 414:98–104.
11. Kanatsu-Shinohara M, Ogonuki N, Inoue K, Miki H, Ogura A, Toyokuni S, Shinohara T. Long-term proliferation in culture and germline transmission of mouse male germline stem cells. Biol Reprod 2003; 69:612–616.
12. Evans MJ, Kaufmann MH. Establishment in culture of pluripotential cells from mouse embryos. Nature 1981; 292:154–156.
13. Martin GR. Isolation of a pluripotent cell line from early mouse embryos cultured in medium conditioned by teratocarcinoma stem cells. Proc Natl Acad Sci U S A 1981; 78:7634–7638.
14. Matsui Y, Zsebo K, Hogan BLM. Derivation of pluripotential embryonic stem cells from murine primordial germ cells in culture. Cell 1992; 70:841–847.
15. Resnick JL, Bixler LS, Cheng L, Donovan PJ. Long-term proliferation of mouse primordial germ cells in culture. Nature 1992; 359:550–551.
16. Barnes D, Sato G. Serum-free culture: a unifying approach. Cell 1980: 22:649–655.
17. Reynolds BA, Weiss S. Generation of neurons and astrocytes from isolated cells of the adult mammalian central nervous system. Science 1992; 255:1707–1710.
18. Okabe M, Ikawa M, Kominami K, Nakanishi T, Nishimune Y. 'Green mice' as a source of ubiquitous green cells. FEBS Lett 1997; 407: 313–319.
19. Xu C, Inokuma MS, Denham J, Golds K, Kundu P, Gold JD, Carpenter MK. Feeder-free growth of undifferentiated human embryonic stem cells. Nat Biotechnol 2001; 19:971–974.
20. Shinohara T, Avarbock MR, Brinster RL. β1- and α6-integrin are surface markers on mouse spermatogonial stem cells. Proc Natl Acad Sci U S A 1999; 96:5504–5509.
21. Keller G, Kennedy M, Papayannopoulou T, Wiles MV. Hematopoietic commitment during embryonic stem cell differentiation in culture. Mol Cell Biol 1993; 13:473–486.
22. Feng L-X, Chen Y, Dettin L, Reijo Pera RA, Herr JC, Goldberg E, Dym M. Generation and in vitro differentiation of a spermatogonial cell line. Science 2002; 297:392–395.
23. Goolsby J, Marty MC, Heletz D, Chiappelli J, Tashko G, Yarnell D, Fishman PS, Dhib-Jalbut S, Bever CT Jr, Trisler D. Hematopoietic progenitors express neural genes. Proc Natl Acad Sci USA 2003; 100: 14926–14931.
24. Yoshida S, Takakura A, Ohbo K, Abe K, Wakabayashi J, Yamamoto M, Suda T, Nabeshima Y. Neurogenin3 delineates the earliest stages of spermatogenesis in the mouse testis. Dev Biol 2004; 269:447–458.
25. Toyooka Y, Tsunekawa N, Akasu R, Noce T. Embryonic stem cells can form germ cells in vitro. Proc Natl Acad Sci U S A 2003; 100: 11457–11462.
26. Silvers WK. Dominant spotting, patch, and rump-white. In: Silvers WK (ed.), The Coat Colors of Mice. New York: Springer; 1979:206–223.
27. Ogawa T, Aréchaga JM, Avarbock MR, Brinster RL. Transplantation of testis germinal cells into mouse seminiferous tubules. Int J Dev Biol 1997; 41:111–122.
28. Kanatsu-Shinohara M, Ogonuki N, Inoue K, Ogura A, Toyokuni S, Honjo T, Shinohara T. Allogeneic offspring produced by male germ line stem cell transplantation into infertile mouse testis. Biol Reprod 2003; 68:167–173.
29. Nagano M, Avarbock MR, Brinster RL. Pattern and kinetics of mouse donor spermatogonial stem cell colonization in recipient testes. Biol Reprod 1999; 60:1429–1436.
30. Kimura Y, Yanagimachi R. Intracytoplasmic sperm injection in the mouse. Biol Reprod 1995; 52:709–720.
31. Svendsen CN, Fawcett JW, Bentlage C, Dunnett SS. Increased survival of rat EGF-generated CNS precursor cells using B27 supplemented medium. Exp Brain Res 1995; 102:407–414.
32. Zhang X, Klueber KM, Guo Z, Lu C, Roisen FJ. Adult human olfactory neural progenitors cultured in defined medium. Exp Neurol 2004; 186:112–123.
33. Anderson R, Schaible K, Heasman J, Wylie CC. Expression of the homophilic adhesion molecule, Ep-CAM, in the mammalian germ line. J Reprod Fertil 1999; 116:379–384.
34. Kanatsu-Shinohara M, Toyokuni S, Shinohara T. CD9 is a surface marker on mouse and rat male germline stem cells. Biol Reprod 2004; 70:70–75.
35. Yoshinaga K, Nishikawa S, Ogawa M, Hayashi S-I, Kunisada T, Fujimoto T, Nishikawa S-I. Role of c-kit in mouse spermatogenesis: identification of spermatogonia as a specific site of c-kit expression and function. Development 1991; 113:689–699.
36. Solter D, Knowles BB. Monoclonal antibody defining a stage-specific mouse embryonic antigen (SSEA-1). Proc Natl Acad Sci U S A 1978; 75:5565–5569.
37. Pesce M, Schöler HR. Oct-4: gatekeeper in the beginnings of mammalian development. Stem Cells 2001; 19:271–278.
38. Brinster RL, Zimmermann JW. Spermatogenesis following male germ-cell transplantation. Proc Natl Acad Sci U S A 1994; 91:11298–11302.
39. Geissler EN, Ryan MA, Housman DE. The dominant white spotting (W) locus of the mouse encodes the *c-kit* proto-oncogene. Cell 1988; 55:185–192.
40. Shinohara T, Avarbock MR, Brinster RL. Functional analysis of spermatogonial stem cells in Steel and cryptorchid infertile mouse models. Dev Biol 2000; 220:401–411.
41. Orwig KE, Shinohara T, Avarbock MR, Brinster RL. Functional analysis of stem cells in the adult rat testis. Biol Reprod 2002; 66:944–949.
42. Saitou M, Barton SC, Surani MA. A molecular program for the specification of germ cell fate in mice. Nature 2002; 418:293–300.
43. Cooke JE, Godin I, Ffrench-Constant C, Heasman J, Wylie C. Culture and manipulation of primordial germ cells. In: Wassarman PM, DePamphilis ML (eds.), Guide to Techniques in Mouse Development. San Diego: Academic Press; 1993:37–58.
44. Palermo G, Joris H, Devroey P, Van Steirteghem AC. Pregnancies after intracytoplasmic injection of single spermatozoon into an oocyte. Lancet 1992; 340:17–18.
45. Kubota H, Avarbock MR, Brinster RL. Culture conditions and single growth factors affect fate determination of mouse spermatogonial stem cells. Biol Reprod 2004; 71:722–731.
46. Dirami G, Ravindranath N, Pursel V, Dym M. Effects of stem cell factor and granulocyte macrophage-colony stimulating factor on survival of porcine type A spermatogonia cultured in KSOM. Biol Reprod 1999; 61:225–230.
47. Creemers LB, den Ouden K, van Pelt AMM, de Rooij DG. Maintenance of adult mouse type A spermatogonia in vitro: influence of serum and growth factors and comparison with prepubertal spermatogonial cell culture. Reproduction 2002; 124:791–799.
48. Ryu B-Y, Orwig KE, Kubota H, Avarbock MR, Brinster RL. Phenotypic and functional characteristics of male germline stem cells in rats. Dev Biol 2004; 274:158–170.
49. Dettin L, Ravindranas N, Hofmann MC, Dym M. Morphological characterization of the spermatogonial subtypes in neonatal mouse testis. Biol Reprod 2003; 69:1565–1571.
50. McLean DJ, Friel PJ, Johnston DS, Griswold MD. Characterization of spermatogonial stem cell maturation and differentiation in neonatal mice. Biol Reprod 2003; 69:2085–2091.
51. Dexter TM, Spooncer E. Growth and differentiation in the hematopoietic system. Annu Rev Cell Biol 1987; 3:423–441.
52. Nagano M, Avarbock MR, Leonida EB, Brinster CJ, Brinster RL. Culture of mouse spermatogonial stem cells. Tissue Cell 1998; 30: 389–397.
53. Nagano M, Ryu B-Y, Brinster CJ, Avarbock MR, Brinster RL. Maintenance of mouse male germ line stem cells in vitro. Biol Reprod 2003; 68:2207–2214.
54. Orwig KE, Avarbock MR, Brinster RL. Retrovirus-mediated modification of male germline stem cells in rats. Biol Reprod 2002; 67:874–879.
55. Kent Hamra F, Schultz N, Chapman KM, Grellhesl DM, Cronkhite JT, Hammer RE, Garbers DL. Defining the spermatogonial stem cell. Dev Biol 2004; 269:393–410.
56. Yomogida K, Yagura Y, Tadokoro Y, Nishimune Y. Dramatic expansion of germinal stem cells by ectopically expressed human glial cell line-derived neurotrophic factor in mouse Sertoli cells. Biol Reprod 2003; 69:1303–1307.
57. Meng X, Lindahl M, Hyvönen ME, Parvinen M, de Rooij DG, Hess MW, Raatikainen-Ahokas A, Sainio K, Rauvala H, Lakso M, Pichel JG, Westphal H, Saarma M, Sariola H. Regulation of cell fate decision of undifferentiated spermatogonia by GDNF. Science 2000; 287: 1489–1493.
58. Tegelenbosch RAJ, de Rooij DG. A quantitative study of spermatogonial multiplication and stem cell renewal in the C3H/101 F1 hybrid mouse. Mutation Res 1993; 290:193–200.

Current Biology 16, 166–172, January 24, 2006 ©2006 Elsevier Ltd All rights reserved DOI 10.1016/j.cub.2005.11.071

Report

Comparison of Gene Expression in Male and Female Mouse Blastocysts Revealed Imprinting of the X-Linked Gene, *Rhox5/Pem*, at Preimplantation Stages

Shin Kobayashi,[1] Ayako Isotani,[1,2] Nathan Mise,[3] Masamichi Yamamoto,[4] Yoshitaka Fujihara,[1,5] Kazuhiro Kaseda,[1] Tomoko Nakanishi,[1,6] Masahito Ikawa,[1] Hiroshi Hamada,[4] Kuniya Abe,[3] and Masaru Okabe[1,2,5,*]

[1] Research Institute for Microbial Diseases
Osaka University
3-1 Yamadaoka
Suita, Osaka 565-0871
Japan

[2] Graduate School of Pharmaceutical Sciences
Osaka University
1-6 Yamadaoka
Suita, Osaka 565-0871
Japan

[3] Technology and Development Team for Mammalian Cellular Dynamics
BioResource Center
RIKEN Tsukuba Institute
3-1-1 Koyadai
Tsukuba Ibaraki 305-0074
Japan

[4] Developmental Genetics Group
Graduate School of Frontier Biosciences
Osaka University
1-3 Yamadaoka
Suita, Osaka 565-0871
Japan

[5] Graduate School of Medicine
Osaka University
2-2 Yamadaoka
Suita, Osaka 565-0871
Japan

Summary

Mammalian male preimplantation embryos develop more quickly than females [1, 2]. Using enhanced green fluorescent protein (EGFP)-tagged X chromosomes to identify the sex of the embryos, we compared gene expression patterns between male and female mouse blastocysts by DNA microarray. We detected nearly 600 genes with statistically significant sex-linked expression; most differed by 2-fold or less. Of 11 genes showing greater than 2.5-fold differences, four were expressed exclusively or nearly exclusively sex dependently. Two genes (*Dby* and *Eif2s3y*) were mapped to the Y chromosome and were expressed in male blastocysts. The remaining two (*Rhox5/Pem* and *Xist*) were mapped to the X chromosome and were predominantly expressed in female blastocysts. Moreover, *Rhox5/Pem* was expressed predominantly from the paternally inherited X chromosome, indicating sex differences in early epigenetic gene regulation.

*Correspondence: okabe@gen-info.osaka-u.ac.jp
[6] Present address: Institute of Applied Biochemistry, University of Tsukuba, Tsukuba Science City, Ibaraki 305-8572, Japan.

Results

Sex-Linked Differential Gene Expression

In mammals, phenotypic gender is normally determined at the time of gonadal differentiation [3]. However, this may not be the sole determinant. For example, male blastocysts develop more quickly than female blastocysts [1, 2], and expression of several genes, such as murine *Xist* [4, 5], bovine *G6PD* [6, 7], *ZFX* [7], *HPRT* [6] and *INF-t* [8], and murine *Zfy* and *Sry* [9], is different in each sex. However, there is no report on global differences in gene expression in male and female blastocysts, largely because of the technical difficulty in sexing many blastocysts quickly and accurately. We overcame this by using a transgenic mouse line in which the X chromosome is tagged with a ubiquitously-expressed EGFP transgene (X^{GFP}) [10–12]. The system is shown in Figures 1A and 1B. Transgenic males ($X^{GFP}Y$) were mated with wild-type females (XX). Only the female embryos (XX^{GFP}) fluoresce green because of the paternally inherited X^{GFP}.

More than 1000 sexed blastocysts were studied. The global gene-expression patterns of male and female blastocysts were compared with the Agilent Mouse Development DNA microarray, which contains 20,371 transcripts (http://lgsun.grc.nia.nih.gov/cDNA/cDNA.html). Three independent experiments were carried out, and Figure 1C shows the normalized results. We identified 591 differentially expressed genes (blue spots); three hundred and eleven were expressed to a higher degree in female blastocysts ($p < 0.01$), and 280 were expressed to a higher degree in males ($p < 0.01$). Most of the differences were 2-fold (200%) or less (Figure 1C).

Of seven genes previously reported to be expressed differentially in male and female blastocysts of the cow and mouse [4–9], three were not represented in this microarray and one was not expressed in the mouse, leaving three candidate genes (*Xist, G6pd, and Hprt*) available for analysis. These were all significantly differently expressed by sex and are listed in Table 1.

Genes showing more than a 2.5-fold (250%) difference in expression (indicated by numbers in Figure 1C and Tables 1 and 2) were reexamined for their expression by reverse transcriptase polymerase chain reaction (RT–PCR) with blastocysts sexed by X^{GFP}. Of these, *Xist* and *Rhox5/Pem* on the X chromosome were predominantly expressed in females, whereas *Dby* and *Eif2s3y* on the Y chromosome were exclusively expressed in males (Figure 2). The same results were obtained with wild-type blastocysts not expressing EGFP (Figure S1 in the Supplemental Data available with this article online).

Verification of Imprinting of the *Rhox5/Pem* Gene

Because *Rhox5/Pem* is located on the X chromosome and is predominantly expressed in females, we

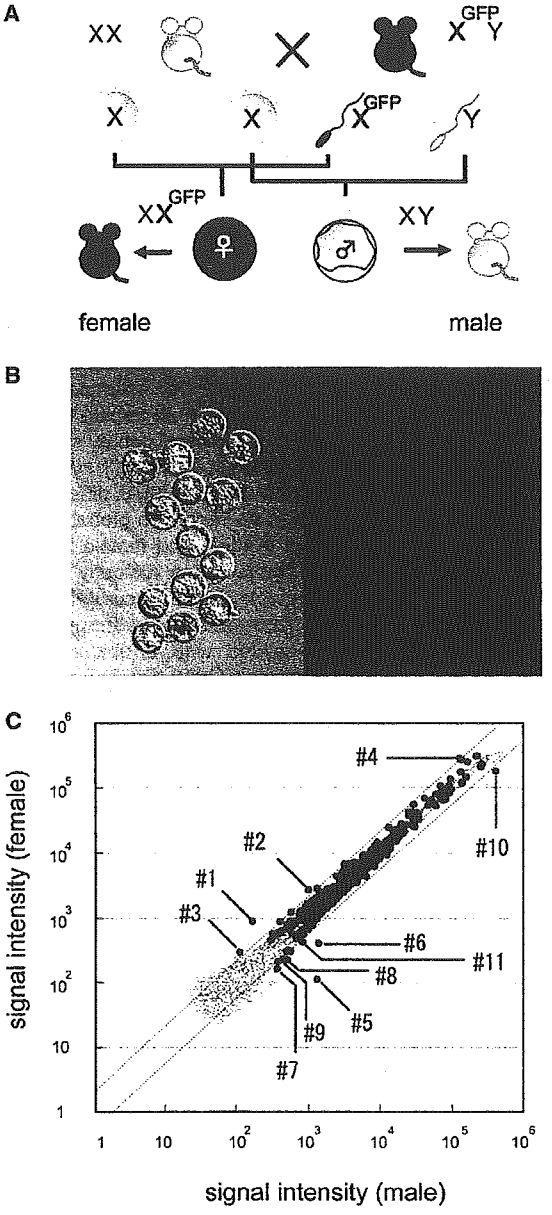

Figure 1. Screening of Differentially Expressed Genes between Sexes at the Preimplantation Stage

(A) The scheme of a X^{GFP} sexing system.

(B) Blastocysts at 3.5 dpc. Only female embryos become green. (Left: bright field. Right: dark field).

(C) Expression profiling of 20K genes between nonfluorescent male and fluorescent female blastocysts. For each gene, average signal intensity is displayed on a scatter plot. Genes that showed significantly different expression levels between females and males at the 1% significance level ($p < 0.01$; the complete description of the statistical methods is available in the technology section of the Rosetta Biosoftware website, http://www.rosettabio.com/tech/default.htm) are displayed as blue spots, and the others are displayed as gray spots. The numbered genes were re-examined for their expression by RT–PCR. Dotted lines indicate 2.0-fold (200%) expression differences.

examined whether it is imprinted, like the *Xist* gene [4, 5]. To distinguish paternal from maternal expression, we produced inter-subspecific F1 mice by crossing *M. m. musculus* (C57BL/6;B6) with *M. m. molossinus* (JF1/Ms;JF1). A DNA polymorphism in the 3′-UTR of the *Rhox5/Pem* gene (Figure 3A) is detectable by restriction fragment length polymorphism (RFLP) analysis with BsrBI. This was used to analyze the active allele in F1 blastocysts derived from mating between C57BL/6 females and JF1/Ms males (B6 × JF1) and the reciprocal cross of JF1/Ms females with C57BL/6 males (JF1 × B6). The RT-PCR products (Figure 3B) clearly show that the gene was predominantly expressed from the paternally inherited X chromosome.

Because early preimplantation-stage embryos already show dosage compensation via inactivation of the paternal X chromosome (Xp) [13–15], we examined whether there was expression of the paternal allele of *Rhox5/Pem* from the 2 cell stage to the blastocyst in embryos from the *M. m. musculus* × *M. m. molossinus* crosses. Figure 3C shows that the gene was expressed predominantly from Xp after the 8 cell stage to the blastocyst stage. This indicated that *Rhox5/Pem* escaped Xp inactivation.

Rhox5/Pem expression levels in male and female post-implantation stages were also examined in embryos at 5.5, 6.5, and 7.5 days post-coitum (dpc) by whole-mount in situ hybridization (Figure 4). Despite the predominant expression in female blastocysts, *Rhox5/Pem* was expressed in both male and female later-stage embryos: not in the epiblasts, but in extraembryonic ectoderm (ExE) and visceral endoderm (VE). When the expressed allele was examined in inter-subspecific crosses, *Rhox5/Pem* was expressed predominantly as the maternal allele in the 7.5 dpc embryos (Figure 3C, right panel).

Discussion

In eutherian mammals, male preimplantation embryos develop more rapidly than females in a number of species, such as the mouse [1, 2], cow [16, 17], human [18], sheep [19], and pig [20]. These differences precede gonadal sex commitment. Here we found minor but statistically significant sex differences in the expressions of nearly 600 genes. These may have arisen from slight differences in developmental stages between the male and female blastocysts, so we cannot conclude that all are associated with sex differentiation. However, we have demonstrated here that at least four genes are certainly expressed differently, not by stage but by sex. We presume that the actual number of genes involved in such sex differences is likely to exceed the small number of previously reported genes [4–9].

Figure 5 indicates the chromosomal distribution of the genes that are differentially expressed by sex. There was no obvious tendency in the distribution of male upregulated genes, whereas there were apparently more female upregulated genes on the X chromosome. When we plotted 212 of these X-linked genes on the X chromosome, most of the variance in expression remained within the range of $1 \leq FC \leq 2$ (Figure S2). These included previously reported female upregulated genes such as *G6pd* and *Hprt* (Table 1, lower row). This slight differential

Table 1. Upregulated Genes in Female Blastocysts

Number[a]	Gene Name	Accession Number	Map Position	N-Fold Change	*p* Value	Intensity (Male)	Intensity (Female)
1	*Xist*[b]	K0418D06-3	X	2.8	4.9×10^{-6}	242	841
2	*Rhox5/Pem*	G0109E12-3	X	2.6	6.3×10^{-28}	1323	3372
3	*EST*	J0030A03-3	X	2.6	4.4×10^{-3}	133	320
4	*EST*	H3075D02-3	8	2.5	4.6×10^{-12}	161060	399351
	G6pd[b]	G0120A12-3	X	1.2	1.5×10^{-3}	2412	2801
	Hprt[b]	H3152G02-3	X	1.5	2.0×10^{-33}	3255	5038

All genes showing more than a 2.5-fold (250%) change in expression level are listed in the upper part of the table.
[a] Numbers correspond to those indicated in Figure 1C.
[b] Genes that were previously reported to be differently expressed.

Table 2. Upregulated Genes in Male Blastocysts

Number[a]	Gene Name	Accession Number	Map Position	N-Fold Change	*p* Value	Intensity (Male)	Intensity (Female)
5	*Dby*	L0814A11-3	Y	−14.8	0	1593	106
6	*Eif2s3y*	H3079H10-3	Y	−3.9	5.0×10^{-26}	1680	460
7	*1110038H03Rik*	C0508G12-3	12	−3.2	7.2×10^{-3}	428	185
8	*EST*	C0282H03-3	17	−3.1	6.0×10^{-4}	584	254
9	*1700019B01Rik*	J0408D11-3	7	−2.7	6.5×10^{-3}	514	259
10	*2310061F22Rik*	J0041H02-3	8	−2.7	1.1×10^{-13}	579807	212643
11	*EST*	L0864B07-3	3	−2.5	4.2×10^{-3}	984	478

All genes for which the change in expression level is less than −2.5-fold are listed.
[a] Numbers correspond to those indicated in Figure 1C.

expression of many X-linked genes may be attributable to incomplete X inactivation or to the reactivation of X-linked genes in epiblast cells.

Many of the genes showing differential expression between sexes were linked to the X chromosome, but only two genes were linked to the Y chromosome. More are likely to be present because some Y-linked genes (*Sry* and *Zfy*) that are expressed in blastocysts were not on our microarray. Other known Y-linked genes on the array are listed in Table S1. However, we clearly detected differential expression of *Dby* and *Eif2s3y*. Because the Y chromosome may accelerate growth of preimplantation mouse embryos, whereas paternally derived X chromosomes or double X chromosomes retard it [21–24], our findings may help elucidate these phenomena.

As with the *Xist* gene, *Rhox5/Pem* was predominantly expressed from the paternally derived X chromosome in the blastocyst. This is a member of a homeobox gene cluster that is mainly expressed in reproductive tissues such as those of the testis, ovary, and placenta, which may play a role in controlling the development of these organs [25]. At present we have no information on the mechanism that enables preferential expression of the paternal *Rhox5/Pem* allele from the 8 cell to the blastocyst stage, when the paternal X is thought to be inactivated, or how the subsequent switch to expression of the maternal allele is brought about. Further experiments are needed to address these issues. However it is known that some imprinted genes show complicated expression patterns. One example is mouse *Grb10*, which shows paternal expression in the brain and maternal expression in other tissues [26, 27]. It is not clear if this imprinting of *Rhox5/Pem* disappeared after implantation, but the expression pattern shown in Figure 3C suggests stage-specific imprinting of this gene.

Using gene targeting, MacLean et al. showed that *Rhox5/Pem* null males were subfertile with reduced sperm count and decreased sperm motility [25]. However, they did not report the effect of gene disruption on embryonic development. It would be worthwhile to examine the early embryonic development between male- and female-targeted mice. However, *Rhox5* is part

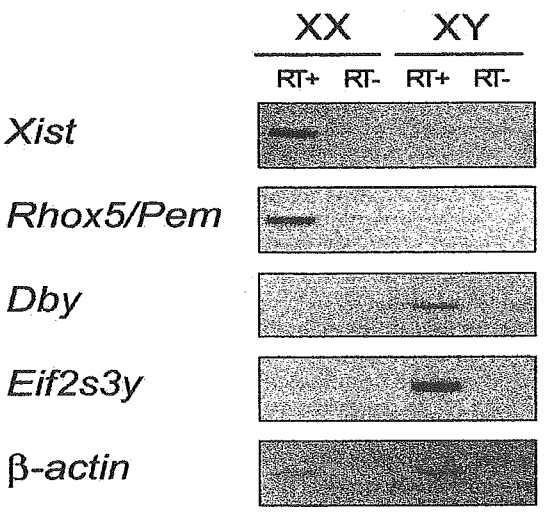

Figure 2. RT-PCR Analysis of Differentially Expressed Genes

Genes showing expression differences of more than 2.5-fold (250%) (see Tables 1 and 2) were chosen, and RT–PCR allowed the differential expression of the genes to be re-examined. Among these genes, four (*Xist, Rhox5/Pem, Dby,* and *Eif2s3y*) showed obvious differences. It should be noted that very weak expression of *Xist* and *Rhox5/Pem* was detected in male blastocysts when additional PCR cycles were carried out.

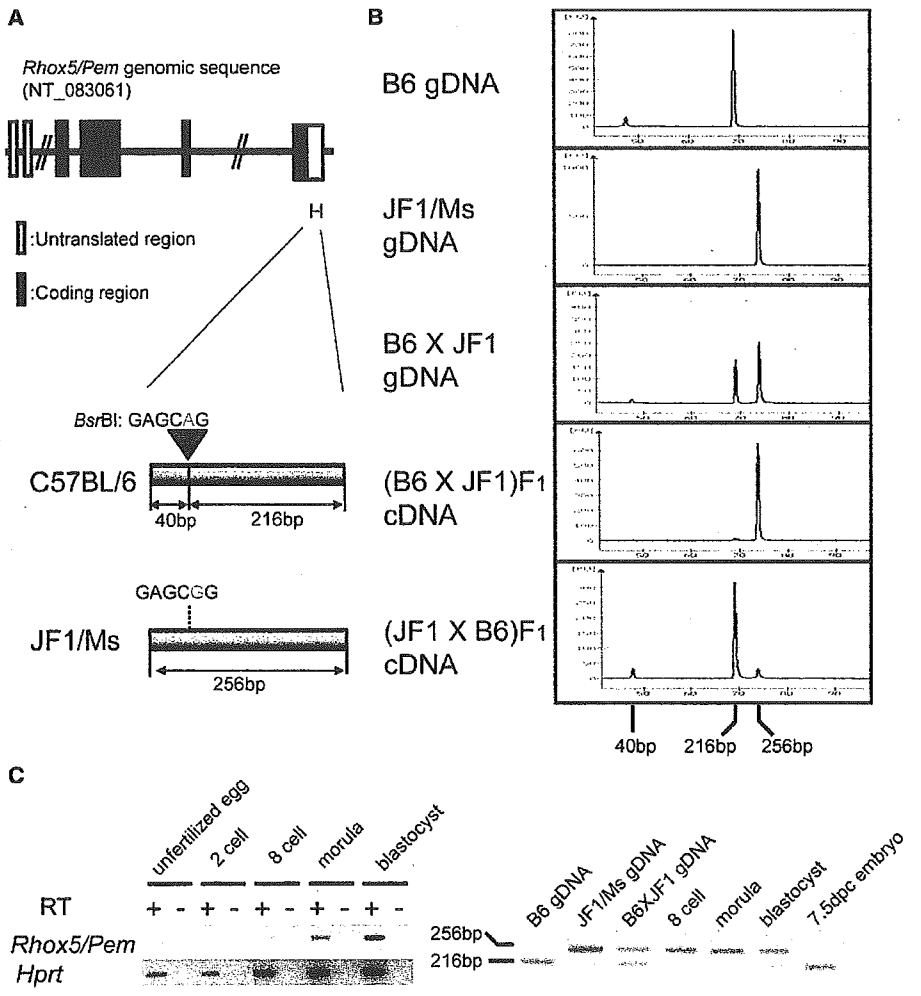

Figure 3. Verification of the *Rhox5/Pem* Gene Imprinting

(A) The single-nucleotide polymorphism detected in C57BL/6;B6 (*M. m. musculus*) and JF1/Ms;JF1 (*M. m. molossinus*) is shown. The BsrBI site (GAGCAG) in the B6 allele was changed to GAGCGG in the JF1 allele. These alleles could be distinguished by digestion with BsrBI; 40 bp and 216 bp digested PCR fragments appeared in the B6 sample, whereas a 256 bp undigested PCR product was seen in the JF1/Ms samples.

(B) Predominant expression of *Rhox5/Pem* from paternal X chromosome was determined by RT–PCR and RFLP analysis with inter-subspecific hybrid mice F1 progenies.

(C) Imprinted expression of *Rhox5/Pem* at early embryonic stages. The expression of *Rhox5/Pem* was examined in unfertilized eggs (B6) and at 2 cell, 8 cell, morula, and blastocyst stages (B6×JF1) (left panel). Allelic expression of *Rhox5/Pem* was analyzed in B6 × J F1 embryos (8 cell, morula, blastocyst, and 7.5 dpc embryonic stages; right panel).

of a family (*Rhox1-12*) whose members might compensate for loss of the *Rhox5/Pem* function. All 12 *Rhox* genes are contained within an approximately 0.7 Mb segment of the X chromosome, and expression analysis of the 12 *Rhox* genes in male and female blastocysts revealed that *Rhox9/Psx2* was also predominantly expressed in females, as with *Rhox5/Pem*. This suggests an imprinted cluster near the *Rhox5/Pem* gene.

Other X-linked imprinted genes (*Xlr3b, Xlr4b,* and *Xlr4c*) have been reported [28, 29], and their expression levels are 5–6 times higher in the developing brain of males than in females. However, *Rhox5/Pem* reported here is paternally expressed, whereas *Xlr* genes are maternally expressed. This finding of imprinted *Rhox5/Pem* indicates epigenetic differences between male and female embryos as early as the preimplantation stage. X-linked imprinted genes in general appear to affect the developmental delay of XO embryos and may be associated with later cognitive dysfunction, if they are mutated [24, 30, 31]. Thus, studies on the potential imprinted regions of *Xlr* genes and *Rhox5/Pem* may provide new insights into imprinting-related disorders.

Conclusions

Nearly 600 genes were differentially expressed between male and female blastocysts. Among these, *Xist* and *Rhox5/Pem* were expressed predominantly in females, and *Dby* and *Eif2s3y* were exclusively expressed in males. Moreover, *Rhox5/Pem* is an imprinted gene expressed from the paternally derived X chromosome, indicating epigenetic sex differences as early as the preimplantation stage.

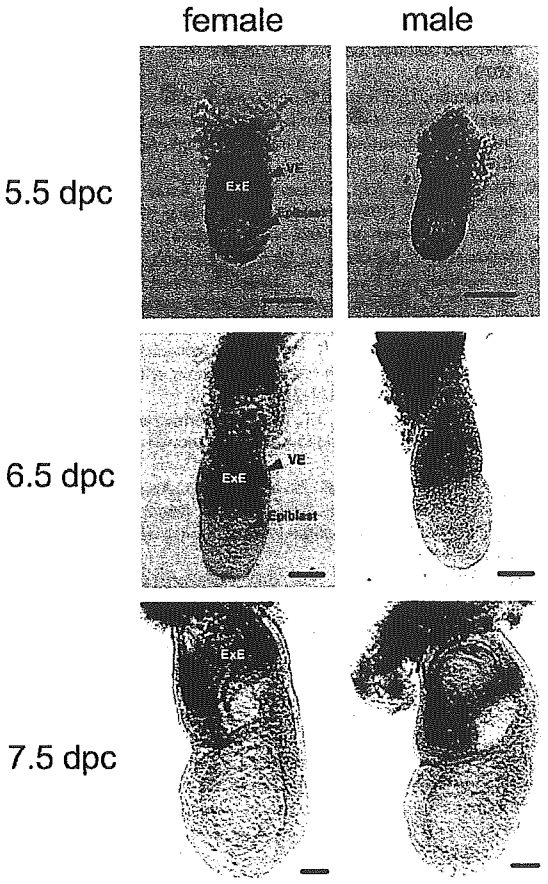

Figure 4. Expression of *Rhox5/Pem* in 5.5, 6.5, and 7.5 dpc Male and Female Embryos

No obvious differences were detected. *Rhox5/Pem* expression was detected in extraembryonic ectoderm (ExE) and visceral endoderm (VE), but not in the epiblast at 5.5 or 6.5 dpc. The expression was also detected in extraembryonic ectoderm (ExE), but not in epiblast, at 7.5 dpc. The scale bar represents 50 μm.

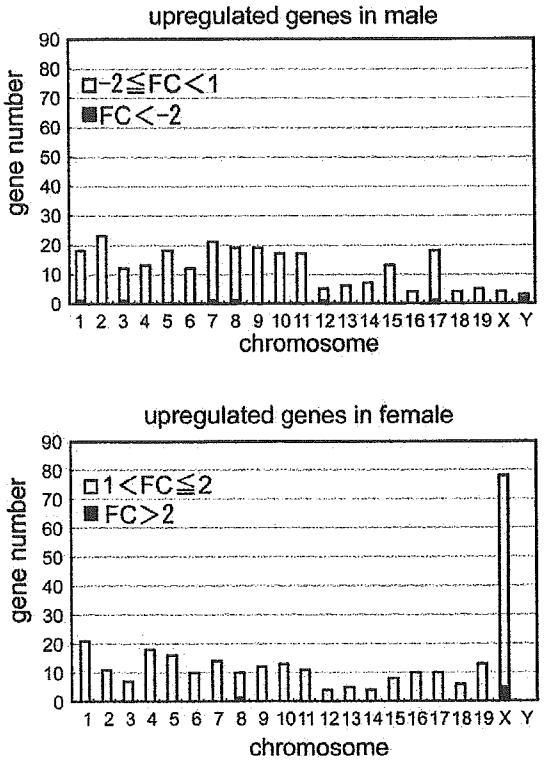

Figure 5. The Chromosomal Distribution of Differentially Expressed Genes

The upper and lower panels show upregulated genes in males and females, respectively. Open and closed bars correspond to the value of n-fold changes as shown in the figures. $p < 0.01$. The calculation methods were the same as those described in the legend for Figure 1C.

Experimental Procedures

Animals

The handling and surgical manipulation of all experimental animals were carried out according to the guidelines of the Committee on the Use of Live Animals in Teaching and Research of Osaka University. The strain B6C3F1 TgN (act EGFP) Osb CX-38 (G38) described previously [11] was used as an EGFP-expressing transgenic mouse line to distinguish between male and female embryos.

Blastocyst Collection and RNA Extraction

Eight-week-old B6C3F$_1$ female mice were superovulated with 5 IU of pregnant mare serum gonadotropin (PMSG) followed by 5 IU of human chorionic gonadotropin (hCG) 48 hr later and were mated with $X^{GFP}Y$ male mice. Four-cell-stage embryos were collected from the oviducts 55 hr after the hCG injection, placed in kSOM, and incubated in a humidified atmosphere of 5% CO_2 in air at 37°C for an additional 38 hr. We separated male (EGFP-negative) and female (EGFP-positive) embryos at the blastocyst stage by observing green fluorescence under a dissection microscope. RNA samples were prepared from sexed blastocysts with ISOGEN (NIPPON GENE Inc., Japan), which is based on acid guanidine thiocyanate-phenol-chloroform extraction. To verify differential gene expression in non-transgenic embryos in vivo, we obtained wild-type C57BL/6 blastocysts from the uterus of superovulated C57BL/6 females mated with wild-type C57BL/6 males 92 hr after hCG injection. Genomic DNA and RNA were extracted from individual blastocysts. Male and female blastocysts were pooled separately after sex determination PCR with the following *Ube1x* primers: 5′-TGGTCTGGACCC AAACGCTGTCCACA-3′ and 5′-GGCAGCAGCCATCACATAATCCA GATG-3′ [32]. For each independent experiment, 30–40 wild-type blastocysts were sexed and pooled samples were used for expression analysis.

Comparative Expression Analysis with DNA Microarray

This is described in the GEO database of NCBI (http://www.ncbi.nlm.nih.gov/projects/geo/). The GEO accession number is GSE2934.

RT-PCR of Candidate Genes for Sexually Dimorphic Expression

Reverse transcription was carried out with the pooled total RNA extracted from 100 blastocysts via Superscript RT (Invitrogen). One hundredth of the resulting cDNA samples was amplified by PCR with *ExTaq* DNA polymerase (TaKaRa). Reaction mixtures contained 1× *ExTaq* buffer, 2.5 mM dNTP, 40 pmol of primers, and 1.25 units of *ExTaq* in a final reaction volume of 50 μl. The amplification conditions were 1 min at 96°C, followed by 30–33cycles for *Xist*, *Rhox5/Pem*, *Dby*, and *Eif2s3y* and 24 cycles for *β-actin*. Cycles were 96°C for 15 s, 65°C for 30 s, and 72°C for 30 s, with a final 1 min extension at 72°C. Primer sets were as follows: 5′-AAGTGTGACGTTGACATC CG-3′ and 5′-GATCCACATCTGCTGGAAGG-3′ for *β-actin*, 5′-CT CATCCTCATGTCTTCTCCG-3′ and 5′-GATTCCAGATAGACAGGCT GG-3′ for *Xist*, 5′-AGAGATGAGCAAGGTGCACA-3′ and 5′-CGAAC CTAGAGCCCTGGAG-3′ for *Rhox5/Pem*, 5′-CGACCATATCTTCCAT TTTCC-3′ and 5′-GCCTGGACCAGCAATTTGTTG-3′ for *Dby*, 5′-GC

CATTTCTGGTGTTCACACTG-3′ and 5′-CATAAGCTTCCCTTCTC CGTC-3′ for *Eif2s3y*. PCR primers for *Dby* and *Eif2s3y* were from [33]. All PCR reactions were repeated at least once. The same PCR conditions were used for examining the wild-type blastocysts, except the amount of starting material (30–40 blastocysts) was different.

Verification of Imprinting

Two reciprocal F_1 hybrid blastocysts, (C57BL/6 × JF1) F_1 and (JF1 × C57BL/6) F_1, were produced by an in vitro fertilization (IVF) method. In each experiment at least 30 blastocysts were sexed with a PCR-based method as described above, and blastocysts were pooled according to their sex. One third of the resulting cDNA samples derived from pooled RNAs were amplified by PCR with the above primers. To verify the imprinting status of *Rhox5/Pem*, we digested amplified PCR products with the BsrBI restriction enzyme and separated them by using an Agilent Bio Analyzer 2100 (Agilent). The allelic expression of *Rhox5/Pem* in 2 cell, 8 cell, and morula stages were analyzed with non-sexed C57BL/6 × JF1 pooled samples (20–50 pooled embryos) by RFLP analysis. Embryos (7.5 dpc) were sexed by PCR as described above; six females were pooled, and expression was analyzed. We carried out duplicate RT-PCR and RFLP analyses.

In Situ Hybridization and Histology

Mouse embryos were staged on the basis of their morphology [34]. Whole-mount in situ hybridization was performed as described in our previous paper [35]. The RNA probes encompass nucleotides 1–431 of *Rhox5/Pem* (NM_008818), and this sequence is specific to *Rhox5/Pem*.

Supplemental Data

Supplemental Data are available with this article online at http://current-biology.com/cgi/content/full/16/2/166/DC1/.

Acknowledgments

This work was supported by a Grant-in-Aid for Scientific Research from The Ministry of Education, Culture, Sports, Science, and Technology and by the 21st Century COE program from the Ministry of Education, Culture, Sports, Science, and Technology of Japan.

Received: July 13, 2005
Revised: November 7, 2005
Accepted: November 25, 2005
Published: January 23, 2006

References

1. Tsunoda, Y., Tokunaga, T., and Sugie, T. (1985). Altered sex ratio of live young after transfer of fast- and slow-developing mouse embryos. Gamete Res. *12*, 301–304.
2. Valdivia, R.P., Kunieda, T., Azuma, S., and Toyoda, Y. (1993). PCR sexing and developmental rate differences in preimplantation mouse embryos fertilized and cultured in vitro. Mol. Reprod. Dev. *35*, 121–126.
3. Jost, A. (1970). Hormonal factors in the sex differentiation of the mammalian foetus. Philos. Trans. R. Soc. Lond. B Biol. Sci. *259*, 119–130.
4. Hartshorn, C., Rice, J.E., and Wangh, L.J. (2002). Developmentally-regulated changes of *Xist* RNA levels in single preimplantation mouse embryos, as revealed by quantitative real-time PCR. Mol. Reprod. Dev. *61*, 425–436.
5. Kay, G.F., Barton, S.C., Surani, M.A., and Rastan, S. (1994). Imprinting and X chromosome counting mechanisms determine *Xist* expression in early mouse development. Cell *77*, 639–650.
6. Gutierrez-Adan, A., Oter, M., Martinez-Madrid, B., Pintado, B., and De La Fuente, J. (2000). Differential expression of two genes located on the X chromosome between male and female in vitro-produced bovine embryos at the blastocyst stage. Mol. Reprod. Dev. *55*, 146–151.
7. Peippo, J., Farazmand, A., Kurkilahti, M., Markkula, M., Basrur, P.K., and King, W.A. (2002). Sex-chromosome linked gene expression in in-vitro produced bovine embryos. Mol. Hum. Reprod. *8*, 923–929.
8. Larson, M.A., and Kubisch, H.M. (1999). The effects of group size on development and interferon-tau secretion by in-vitro fertilized and cultured bovine blastocysts. Hum. Reprod. *14*, 2075–2079.
9. Zwingman, T., Erickson, R.P., Boyer, T., and Ao, A. (1993). Transcription of the sex-determining region genes *Sry* and *Zfy* in the mouse preimplantation embryo. Proc. Natl. Acad. Sci. USA *90*, 814–817.
10. Hadjantonakis, A.K., Gertsenstein, M., Ikawa, M., Okabe, M., and Nagy, A. (1998). Non-invasive sexing of preimplantation stage mammalian embryos. Nat. Genet. *19*, 220–222.
11. Nakanishi, T., Kuroiwa, A., Yamada, S., Isotani, A., Yamashita, A., Tairaka, A., Hayashi, T., Takagi, T., Ikawa, M., Matsuda, Y., et al. (2002). FISH analysis of 142 EGFP transgene integration sites into the mouse genome. Genomics *80*, 564–574.
12. Okabe, M., Ikawa, M., Kominami, K., Nakanishi, T., and Nishimune, Y. (1997). 'Green mice' as a source of ubiquitous green cells. FEBS Lett. *407*, 313–319.
13. Huynh, K.D., and Lee, J.T. (2003). Inheritance of a pre-inactivated paternal X chromosome in early mouse embryos. Nature *426*, 857–862.
14. Mak, W., Nesterova, T.B., de Napoles, M., Appanah, R., Yamanaka, S., Otte, A.P., and Brockdorff, N. (2004). Reactivation of the paternal X chromosome in early mouse embryos. Science *303*, 666–669.
15. Okamoto, I., Otte, A.P., Allis, C.D., Reinberg, D., and Heard, E. (2004). Epigenetic dynamics of imprinted X inactivation during early mouse development. Science *303*, 644–649.
16. Avery, B., Jorgensen, C.B., Madison, V., and Greve, T. (1992). Morphological development and sex of bovine in vitro-fertilized embryos. Mol. Reprod. Dev. *32*, 265–270.
17. Yadav, B.R., King, W.A., and Betteridge, K.J. (1993). Relationships between the completion of first cleavage and the chromosomal complement, sex, and developmental rates of bovine embryos generated in vitro. Mol. Reprod. Dev. *36*, 434–439.
18. Pergament, E., Fiddler, M., Cho, N., Johnson, D., and Holmgren, W.J. (1994). Sexual differentiation and preimplantation cell growth. Hum. Reprod. *9*, 1730–1732.
19. Bernardi, M.L., and Delouis, C. (1996). Sex-related differences in the developmental rate of in-vitro matured/in-vitro fertilized ovine embryos. Hum. Reprod. *11*, 621–626.
20. Cassar, G., King, W.A., and King, G.J. (1994). Influence of sex on early growth of pig conceptuses. J. Reprod. Fertil. *101*, 317–320.
21. Banzai, M., Omoe, K., Ishikawa, H., and Endo, A. (1995). Viability, development and incidence of chromosome anomalies of preimplantation embryos from XO mice. Cytogenet. Cell Genet. *70*, 273–277.
22. Burgoyne, P.S. (1993). A Y-chromosomal effect on blastocyst cell number in mice. Development *117*, 341–345.
23. Burgoyne, P.S., Thornhill, A.R., Boudrean, S.K., Darling, S.M., Bishop, C.E., and Evans, E.P. (1995). The genetic basis of XX-XY differences present before gonadal sex differentiation in the mouse. Philos. Trans. R. Soc. Lond. B Biol. Sci. *350*, 253–260.
24. Thornhill, A.R., and Burgoyne, P.S. (1993). A paternally imprinted X chromosome retards the development of the early mouse embryo. Development *118*, 171–174.
25. Maclean, J.A., 2nd, Chen, M.A., Wayne, C.M., Bruce, S.R., Rao, M., Meistrich, M.L., Macleod, C., and Wilkinson, M.F. (2005). Rhox: A new homeobox gene cluster. Cell *120*, 369–382.
26. Arnaud, P., Monk, D., Hitchins, M., Gordon, E., Dean, W., Beechey, C.V., Peters, J., Craigen, W., Preece, M., Stanier, P., et al. (2003). Conserved methylation imprints in the human and mouse *GRB10* genes with divergent allelic expression suggests differential reading of the same mark. Hum. Mol. Genet. *12*, 1005–1019.
27. Hikichi, T., Kohda, T., Kaneko-Ishino, T., and Ishino, F. (2003). Imprinting regulation of the murine *Meg1/Grb10* and human *GRB10* genes; roles of brain-specific promoters and mouse-specific CTCF-binding sites. Nucleic Acids Res. *31*, 1398–1406.
28. Davies, W., Isles, A., Smith, R., Karunadasa, D., Burrmann, D., Humby, T., Ojarikre, O., Biggin, C., Skuse, D., Burgoyne, P., et al. (2005). *Xlr3b* is a new imprinted candidate for X-linked

parent-of-origin effects on cognitive function in mice. Nat. Genet. *37*, 625–629.
29. Raefski, A.S., and O'Neill, M.J. (2005). Identification of a cluster of X-linked imprinted genes in mice. Nat. Genet. *37*, 620–624.
30. Jamieson, R.V., Tan, S.S., and Tam, P.P. (1998). Retarded post-implantation development of X0 mouse embryos: Impact of the parental origin of the monosomic X chromosome. Dev. Biol. *201*, 13–25.
31. Skuse, D.H., James, R.S., Bishop, D.V., Coppin, B., Dalton, P., Aamodt-Leeper, G., Bacarese-Hamilton, M., Creswell, C., McGurk, R., and Jacobs, P.A. (1997). Evidence from Turner's syndrome of an imprinted X-linked locus affecting cognitive function. Nature *387*, 705–708.
32. Chuma, S., and Nakatsuji, N. (2001). Autonomous transition into meiosis of mouse fetal germ cells in vitro and its inhibition by gp130-mediated signaling. Dev. Biol. *229*, 468–479.
33. Dewing, P., Shi, T., Horvath, S., and Vilain, E. (2003). Sexually dimorphic gene expression in mouse brain precedes gonadal differentiation. Brain Res. Mol. Brain Res. *118*, 82–90.
34. Downs, K.M., and Davies, T. (1993). Staging of gastrulating mouse embryos by morphological landmarks in the dissecting microscope. Development *118*, 1255–1266.
35. Yamamoto, M., Saijoh, Y., Perea-Gomez, A., Shawlot, W., Behringer, R.R., Ang, S.L., Hamada, H., and Meno, C. (2004). Nodal antagonists regulate formation of the anteroposterior axis of the mouse embryo. Nature *428*, 387–392.

nature medicine

Angiotensin-converting enzyme is a GPI-anchored protein releasing factor crucial for fertilization

Gen Kondoh[1,7,8], Hiromasa Tojo[2], Yuka Nakatani[1], Nobuyasu Komazawa[1], Chie Murata[3], Kazuo Yamagata[4,9], Yusuke Maeda[5], Taroh Kinoshita[5,8], Masaru Okabe[4], Ryo Taguchi[3,8] & Junji Takeda[1,6]

The angiotensin-converting enzyme (ACE) is a key regulator of blood pressure. It is known to cleave small peptides, such as angiotensin I and bradykinin and changes their biological activities, leading to upregulation of blood pressure. Here we describe a new activity for ACE: a glycosylphosphatidylinositol (GPI)-anchored protein releasing activity (GPIase activity). Unlike its peptidase activity, GPIase activity is weakly inhibited by the tightly binding ACE inhibitor and not inactivated by substitutions of core amino acid residues for the peptidase activity, suggesting that the active site elements for GPIase differ from those for peptidase activity. ACE shed various GPI-anchored proteins from the cell surface, and the process was accelerated by the lipid raft disruptor filipin. The released products carried portions of the GPI anchor, indicating cleavage within the GPI moiety. Further analysis by high-performance liquid chromatography–mass spectrometry predicted the cleavage site at the mannose-mannose linkage. GPI-anchored proteins such as TESP5 and PH-20 were released from the sperm membrane of wild-type mice but not in *Ace* knockout sperm *in vivo*. Moreover, peptidase-inactivated E414D mutant ACE and also PI-PLC rescued the egg-binding deficiency of *Ace* knockout sperms, implying that ACE plays a crucial role in fertilization through this activity.

In mammals, more than 200 cell surface proteins with various functions, such as hydroxylation, cellular adhesion and receptor, are anchored to the membrane by a covalently attached GPI moiety[1,2]. GPI deficiency causes developmental abnormalities, failure of skin barrier formation and female infertility in mice, indicating that a GPI anchor is essential for cell integrity[3–5]. Patients with the acquired hematopoietic disorder paroxysmal nocturnal hemoglobinuria have defective biosynthesis of GPI in hematopoietic stem cells[1,2]. The discovery of the *PIGA* gene and its mutations in paroxysmal nocturnal hemoglobinuria has opened the avenue for investigating the mechanisms involved in GPI biosynthesis, although the information on the metabolic system of GPI-anchored proteins is still limited[6,7].

Prions are infectious pathogens that cause fatal neurodegenerative diseases in both human and cattle through the modification of prion protein[8,9]. Because prion protein is a GPI-anchored protein and its release is strictly linked to its pathogenic role[10,11], studies on the general mechanisms and biological meaning of released GPI-anchored protein are necessary to establish new strategies for defeating these incurable neurodegenerative diseases.

To investigate the fate of GPI *in vivo*, we previously developed GPI-anchored enhanced green fluorescent protein (EGFP-GPI) transgenic mice and found a considerable amount of EGFP-GPI in the extracellular fluid[12]. This phenotype prompted us to identify GPI-anchored protein releasing factors, in order to identify new mechanisms of GPI-anchored protein turnover other than the recycling between plasma membrane and endosomes[13,14].

The angiotensin-converting enzyme (ACE) is a well-characterized zinc peptidase that regulates bioactivities of circulating peptides such as angiotensin I and bradykinin as a dipeptidyl carboxypeptidase[15,16], leading to upregulation of blood pressure. Two isoforms of ACE, the somatic and testicular forms, have been characterized and both contain the zinc binding motif HEXXH in the center of the active site[17]. Its peptidase activity is completely abolished by either chelating the zinc ion or exchanging the conserved amino acid residues[18]. Furthermore, ACE inhibitors, which are widely used as antihypertensive agents, specifically bind and compete with substrate peptides at this active site, indicating that the active site of ACE is indispensable for the peptidase activity[19].

Because the molecular size of ACE is rather large (150–180 kDa and 100–110 kDa for somatic and testicular isoforms, respectively), it is conceivable that the enzyme has other undiscovered functions. In this regard, a homolog of ACE, the ACE-2 (ref. 20), which is also a zinc peptidase and acts as an antagonist for ACE peptidase function, was recently found to act as a receptor for the virus that causes severe acute respiratory syndrome (SARS)[21]. In this report, we describe a new function for ACE; it has a GPI-anchored protein releasing activity and that it has a crucial role in fertilization through this activity.

[1]Department of Social and Environmental Medicine and [2]Department of Biochemistry and Molecular Biology, Graduate School of Medicine, Osaka University, Suita, 2-2 Yamadaoka, Osaka 565-0871, Japan. [3]Department of Metabolome, Graduate School of Medicine, The University of Tokyo, 7-3-1 Hongo, Bunkyo-ku, Tokyo, 113-0033, Japan. [4]Genome Information Research Center, and [5]Research Institute for Microbial Diseases, Osaka University, 3-1 Yamadaoka, Suita, Osaka 565-0871, Japan. [6]Center for Advanced Science and Innovation, Osaka University, 2-1 Yamadaoka, Suita, Osaka 565-0871, Japan. [7]Present address: Laboratory of Animal Experiments for Regeneration, Institute for Frontier Medical Sciences, Kyoto University, Japan. [8]Present address: CREST, Japan Science and Technology Society, 53 Syogoin-Kawahara-cho, Sakyo-ku, Kyoto 606-8507, Japan. [9]Present address: Institute of Applied Biochemistry, University of Tsukuba, 1-1-1 Tennoudai, Tsukuba Science City, Ibaraki 305-8572, Japan. Correspondence should be addressed to G.K. (kondohg@frontier.kyoto-u.ac.jp) or J.T. (takeda@mr-envi.med.osaka-u.ac.jp).

Published online 23 January 2005; doi:nm10.1038/nm1179

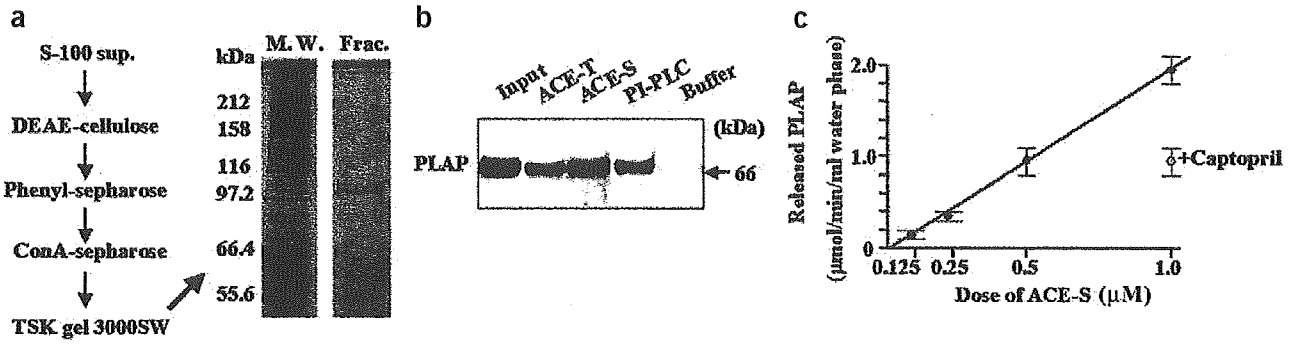

Figure 1 ACE acts as a GPI anchored protein–releasing factor. (**a**) A single 100-kDa band isolated by the TSK gel 3000SW column was subjected to SDS-PAGE and silver stained. (**b**) Immunoblotting of released PLAP from reaction with purified ACE-t, ACE-S, PI-PLC or vehicle alone (Buffer). 'Input' indicates substrate of the reaction. The size of the products released by ACE and PI-PLC was similar to that of the substrate. (**c**) Dose dependence of ACE-S GPIase activity. The results of experiments in which captopril was applied are also indicated. Values are mean ± s.d., $n = 3$.

RESULTS

Identification of ACE as a GPI-anchored protein releasing factor

First, we established an assay system to monitor the GPIase activity, taking advantage of the temperature-dependent phase separation of the aqueous TritonX-114 solution, which can separate water-soluble released proteins (products) from detergent-soluble GPI-anchored proteins (substrates) at 37 °C. When GPI-anchored proteins are deprived of their lipid moiety, they shift from the detergent-soluble phase to the water-soluble phase. This assay system was used for monitoring GPIase activity through purification. We examined this activity in various organs using both EGFP-GPI and the placental alkaline phosphatase (PLAP) as probes for GPI-anchored proteins and found a substantial activity in testicular germ cells (see **Supplementary Fig. 1** online). We also examined the expression of *Gpld1*, the gene that encodes a GPI anchor–cleaving enzyme in mammals[22,23], in various tissues. Because testicular germ cells do not express *Gpld1*, this activity may be compensated by other factors (**Supplementary Fig. 2** online). Therefore, we decided to identify the molecular entity of the enzyme responsible for GPIase activity in these cells. Using serial liquid chromatography that started from detergent-soluble fraction of mouse testicular germ cells, we purified a 100-kDa protein and subsequently identified it as ACE by proteomics analysis (**Fig. 1a**, **Table 1** and **Supplementary Fig. 3** online). To confirm that this GPIase activity involved ACE, we performed a similar assay using either a recombinant product of testicular isoform ACE (ACE-t; **Supplementary Fig. 4** online) or a commercially available rabbit ACE (ACE-S) and purified PLAP as substrate (**Supplementary Fig. 5** online). The products released by this activity had the same size as those of bacterial phosphatidylinositol-specific phospholipase (PI-PLC), a commonly used GPI anchor–cleaving enzyme, implying that this activity cleaves GPI-anchored protein located in proximity to the cleavage site of PI-PLC (**Fig. 1b**). Similar activities were shown by both molecules in a dose-dependent manner (**Fig. 1c**, data not shown), confirming that ACE was responsible for GPIase activity and did not require other factors for the action.

Characterization of ACE GPIase activity

To examine whether the ACE GPIase activity is identical to the PI-PLC activity, we used several PI-PLC inhibitors, such as myo-inositol, inositol monophosphate and antibody specific for PI-PLC, as well as PLC inhibitors such as A23187, U-73122 and C48/80 on ACE GPIase assay. None of these compounds had any inhibitory effects, even when used at a high dose (100 mM each), indicating that ACE GPIase activity is not an endogenous PI-PLC-like activity (data not shown).

We also assessed the effect of ACE-specific inhibitors, such as captopril and lisinopril, which bind to the catalytic center with ligation of its thiol to the zinc ion and completely inhibit the peptidase activity, but found only a minor inhibitory effect on the GPIase assay (**Fig. 1c**, 1×10^{-3} M captopril produced 40% inhibition and data not shown). Moreover, we assessed the effect of chloride ion, which activates the peptidase activity of ACE[15,16], but found no effects on the GPIase activity (data not shown).

We then assessed the metal requirement for GPIase activity. First, ethylenediaminetetraacetic acid (EDTA), which can remove various metal ions from proteins, was added at different doses to the PLAP conversion assay. Because EDTA has some inhibitory effects on PLAP enzyme action[24], immunoblotting was performed using antibody specific for PLAP to check for PLAP release. GPIase activity was inhibited by 1 mM of EDTA but not by an amount (10% less) at which peptidase activity was considerably inhibited (**Fig. 2a**). We also assessed the effects of other metal chelating reagents, such as *trans*-1,2-diaminocyclohexane-N, N, N′, N′-tetraacetic acid (CyDTA) and ethylene glycol bis (beta-aminoethyl ether)-N, N, N′, N′-tetraacetic acid (EGTA).

Table 1 Purification of GPI-anchored protein releasing activity from male germ cells

Column	Volume (ml)	Total protein (mg)	Total activity (AU)*	Specific activity (U/mg protein)	Fold purification
S-100 sup.	393	19,100	336,160	18	1.0
DEAE-cellulose	8	228	14,410	63	3.5
Phenyl-sepharose	8	212	17,596	83	4.6
Con-A-sepharose	1	6	6,100	1,017	56.5
TSK gel 3000SW	1	1	2,500	2,500	138.9

The membrane-rich fraction of germ cells from mouse testis was solubilized in a buffer containing 1% Triton X-100, centrifuged and the supernatant was collected and subjected to chromatographic fractionation. The PLAP conversion assay was performed on the eluted fractions and the maximum values are used here.

$$\text{*Arbitrary Unit} = \frac{[\text{OD595: sample}] - [\text{OD595: background}]}{[\text{OD595: PI-PLC}] - [\text{OD595: background}]}$$

All reactions were performed using PI-PLC (1.0 IU/ml), the value of which was defined as maximum reaction.

The peptidase activity was vigorously inhibited by 1 mM of each of these reagents, but found no inhibition of GPIase activity. To confirm the difference in GPIase and peptidase activities, we replaced Glu414 with aspartate or replaced both His413 and His417 with lysine in ACE-t (**Supplementary Fig. 4** online), which activates a water nucleophile as a general base or captures a zinc ion, thus becoming essential for peptidase activity[18]. These mutants showed only a trace peptidase activity but retained GPIase activity at a level comparable with that of wild-type ACE-t (**Fig. 2b**). The GPIase activity of H413K-H417K mutant, which cannot capture the zinc ion at the peptidase active site, was also inhibited by high-dose EDTA but not by CyDTA or EGTA (**Fig. 2c**), suggesting that EDTA-induced inhibition of GPIase activity is mediated in a non-metal-chelating manner[25,26] and that the GPIase action of ACE does not require zinc ion. Considered together, these results suggest that the active site element for GPIase activity differ from that for peptidase activity.

ACE sheds various GPI-anchored proteins from the cell surface

To examine whether ACE GPIase activity catalyzes GPI-anchored proteins in intact cells, we developed the F9 cell clone, which stably expressed EGFP-GPI on the cell surface. Although ACE exerted little effect on EGFP-GPI expression, pretreatment of cells with filipin, a commonly used reagent for lipid raft disruption[27], allowed ACE to shed EGFP-GPI from the cell surface (**Fig. 3a,b**). Most of the GPI-anchored proteins are localized and packed in the lipid raft[28–30]. Furthermore, increased accessibility of GPI-anchored proteins to shedding enzyme was observed upon disruption of lipid raft[31]. Because filipin has no pharmacological effects on ACE GPIase activity, as assessed by PLAP conversion assay (data not shown), exogenous ACE seems to be prevented from accessing the substrate molecules by this membrane microstructure. In contrast, both ACE and PI-PLC had no effect on the transmembrane protein E-cadherin, implying that the activity of ACE is unique for GPI-anchored protein shedding. Moreover, ACE displayed both time- and dose-dependent enzymatic characteristics (data not shown).

We examined the effect of this activity on various endogenous GPI-anchored proteins including Sca-1 and Thy-1 in F9 cells; CD59 and the decay-accelerating factor (DAF) in HeLa cells; and prion protein (PrP) and CD59 in HEK293 cells (**Fig. 3c**). All proteins, except transmembrane protein E-cadherin, were efficiently shed but at various degrees. In contrast to F9 cell molecules, GPI-anchored proteins on human cells were readily released from the cell surface without filipin treatment.

ACE cleaves GPI moiety

To determine the ACE cleavage profile on the substrate, we performed the following studies. First, we used radiolabeling to clarify whether the released molecules contained GPI components. We metabolically labeled the F9 cells expressing EGFP-GPI with radioactive phosphate or ethanolamine, both of which could be incorporated into the GPI anchor moiety but not in the EGFP protein. We treated cells with ACE, PI-PLC or mouse glandular kallikrein (mGK), which digests EGFP protein near the carboxy termini (data not shown) and trapped the released products from the supernatants using antibody specific for GFP. Following sodium dodecyl sulfate–polyacrylamide gel electrophoresis (SDS-PAGE) and transfer onto nitrocellulose membrane, we performed autoradiography followed by immunoblotting to detect EGFP-GPI protein. The ACE-released EGFP-GPI was labeled with [^{32}P]-phosphate or [^{3}H]-ethanolamine, but not mGK-treated products, indicating the presence of a portion of GPI anchor structure in the ACE-released molecules (**Fig. 4a**). The radioactivity of released products was about one-third when it was labeled on the phosphate and one-half on the ethanolamine compared with those of PI-PLC-released molecules, suggesting that ACE cleaves GPI anchor between mannoses or at the linkage between phosphate and the third mannose.

We then examined the difference in the cleavage mechanism between ACE and PI-PLC. K562 human erythroleukemia cell line was treated with either enzyme to test the shedding of the surface DAF. Because an additional fatty acylation on the inositol hydroxyl is frequently found on mature GPI anchor[2] and this modification is prominent in K562

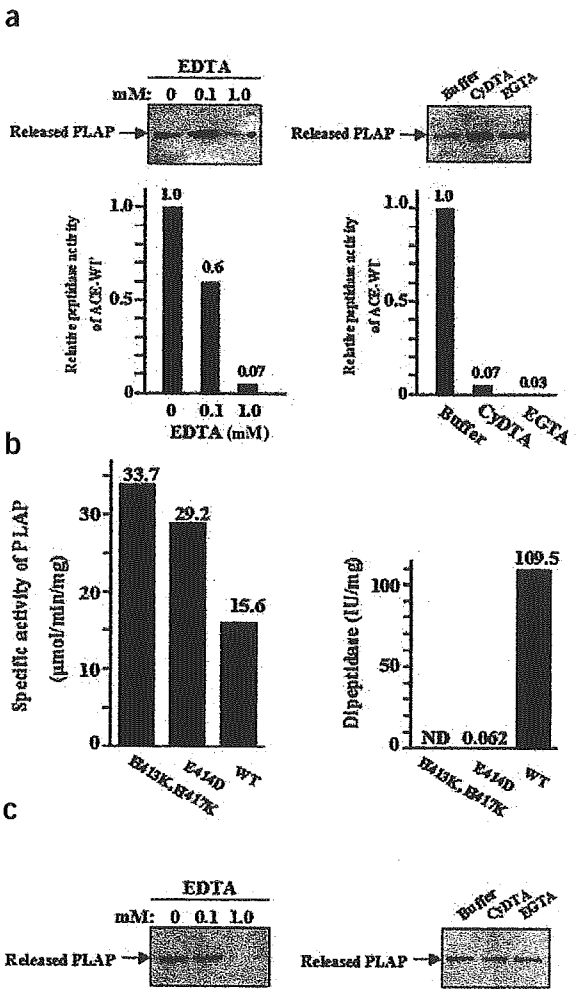

Figure 2 Differences in GPIase and peptidase activities of ACE. (**a**) Effects of metal chelating reagents on the wild-type Ace. EDTA, CyDTA or EGTA was applied to the PLAP conversion assay and the released PLAP was detected by immunoblotting (top). Bottom panels indicate effects of these reagents on the peptidase activity (activity under control condition; *i.e.*, no reagent, was considered 1.0). Dose effect of EDTA on GPIase and peptidase activities. EDTA was applied at 0.1 mM or 1 mM (left). Effects of high dose (1 mM) CyDTA and EGTA on GPIase and peptidase activities (right). Buffer indicates no reagent applied. (**b**) GPIase and peptidase activities of the wild-type (WT), E414D and H413K-H417K mutants. GPIase activity is expressed as released PLAP activity (left). The dipeptidyl carboxypeptidase (Dipeptidase) activity of the same samples (right). ND, not detected. (**c**) Effects of metal chelating reagents on the H413K-H417K mutant. EDTA, CyDTA or EGTA was applied to the PLAP conversion assay and the released PLAP was detected by immunoblotting. Dose effect of EDTA on GPIase activity (left). EDTA was applied at 0.1 mM or 1 mM. Effects of high-dose (1 mM) CyDTA and EGTA on GPIase activity (right).

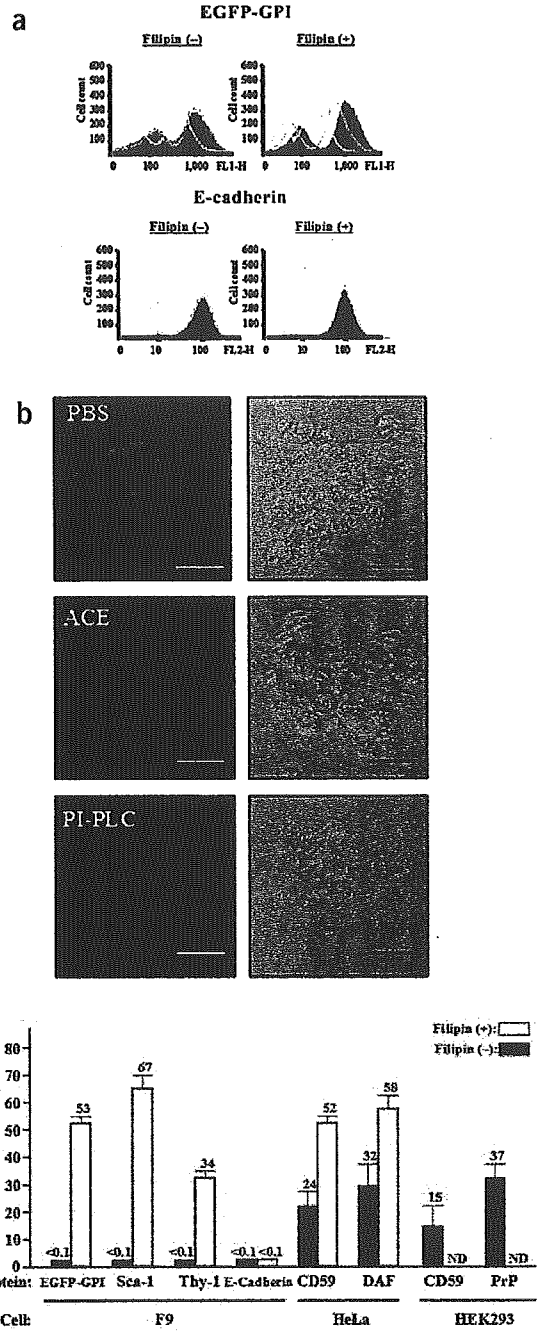

Figure 3 Shedding activity of ACE on the cell surface. (**a**) Expression of EGFP-GPI was examined by FACS analysis. Purple area, ACE (–); green line, ACE (+); yellow line, PI-PLC-treated; black dot, background. (**b**) Expression of EGFP-GPI after ACE or PI-PLC treatment examined by fluorescence microscopy. Note that the fluorescence of Golgi complex remained the same. Magnification, ×200. (**c**) ACE caused shedding of various endogenous GPI-anchored proteins. The amount of ACE used was equivalent to the endogenous ACE activity. Values are mean ± s.d., $n = 3$. ND, not determined.

(ref. 32), resistance to PI-PLC treatment was apparent, whereas ACE considerably shed DAF (**Supplementary Fig. 6** online).

We also attempted to identify the structure of the carboxy-terminal peptides by high-performance liquid chromatography–mass spectrometry with trypsin treatment of the released EGFP-GPI. Under high-peptide coverage, we found a single charged fragment at mass-to-charge ratio (m/3) 660.5, corresponding to the carboxy-terminal peptide LEN, carrying an ethanolamine-phosphate-mannose structure, suggesting that ACE cleaves GPI anchor between the first and second mannose of the GPI moiety (**Fig. 4b**). This conclusion was supported by the fact that its tandem mass spectra showed intense dehydrated ions of $(M + H)^+$ at m/z 642 and less intense ions at m/z 498 that underwent neutral loss of mannose-H_2O. These results suggest that ACE cleaves GPI anchor as an endo-mannosidase, different from PI-PLC cleavage, which is more proximate to the protein.

Rescue of *ACE* knockout sperm by mutant ACE and PI-PLC

The most prominent phenotype of *Ace* knockout mouse is male infertility. Although the physiological parameters of *Ace* knockout sperm, such as number, shape, viability, mobility and rates of capacitation and acrosomal reaction, were not different from those of wild-type sperm, they showed defective sperm-egg binding at the zona pellucida[33,34].

To show a functional ACE GPIase activity *in vivo* and assess its role in fertilization, we first checked the state of GPI-anchored proteins in the sperm. We collected epididymal sperm from both wild-type and *Ace* knockout mice[33] and compared the distribution of GPI-anchored proteins in water-soluble and detergent-soluble fractions. In the sperm, the water-soluble fraction contains soluble ingredients of the acrosome, whereas the detergent-soluble fraction consists of membrane components. Two GPI-anchored proteins, Tesp5 and Ph-20, were examined, because both proteins are released from the sperm during fertilization[35,36]. Immunoblotting showed both Tesp5 and Ph-20 in the water-soluble fraction of wild-type sperm but not in the *Ace* knockout sperm (**Fig. 5a**), implying that ACE participates in converting GPI-anchored proteins from the membrane-bound form to a soluble form.

Finally, we examined the effect of ACE on sperm-egg binding. We prepared epididymal sperm of both genotypes and treated them with either wild-type or peptidase-inactivated ACE (ACE-E414D) or PI-PLC and then incubated them with unfertilized eggs from C57BL/6 mice. These treatments had no effect on wild-type sperm–zona pellucida binding (data not shown). In contrast, treatment with wild-type or ACE-E414D vigorously restored sperm–zona pellucida binding of the *Ace* knockout mice (**Fig. 5b**). Moreover, PI-PLC treatment apparently restored the egg-binding ability of *Ace* knockout sperm to a level comparable with both ACE treatments, confirmed by inhibition with inositol monophosphate, a PI-PLC-specific inhibitor (**Fig. 5c**). Then, we transplanted the wild-type oocytes fertilized with ACE-pretreated knockout sperm into pseudopregnant females to assess their developmental potential. Normal $ACE^{+/-}$ pups were born (**Supplementary Fig. 7 online**). These findings indicate that ACE GPIase activity is crucial for the egg-binding ability of sperm.

DISCUSSION

The major finding of the present study was the discovery that ACE is a GPI-anchored protein releasing factor. Furthermore, this activity of ACE might also be different from that of GPI-PLD, the only enzyme known so far to cleave GPI anchor in mammals[22,23]. It has been reported that GPI-PLD releases GPI-anchored protein only when it is expressed intracellularly in culture cells[23]. In contrast, ACE efficiently released GPI-anchored protein from the cell surface. Because GPI-PLD cleaves GPI anchor at the phosphorus-oxygen bond of the phosphatidylinositol backbone[22], inositol acylation may also prevent completion of GPI-anchored protein release by GPI-PLD. Indeed, GPI-PLD could not release DAF from the intact erythrocyte[37]. In contrast,

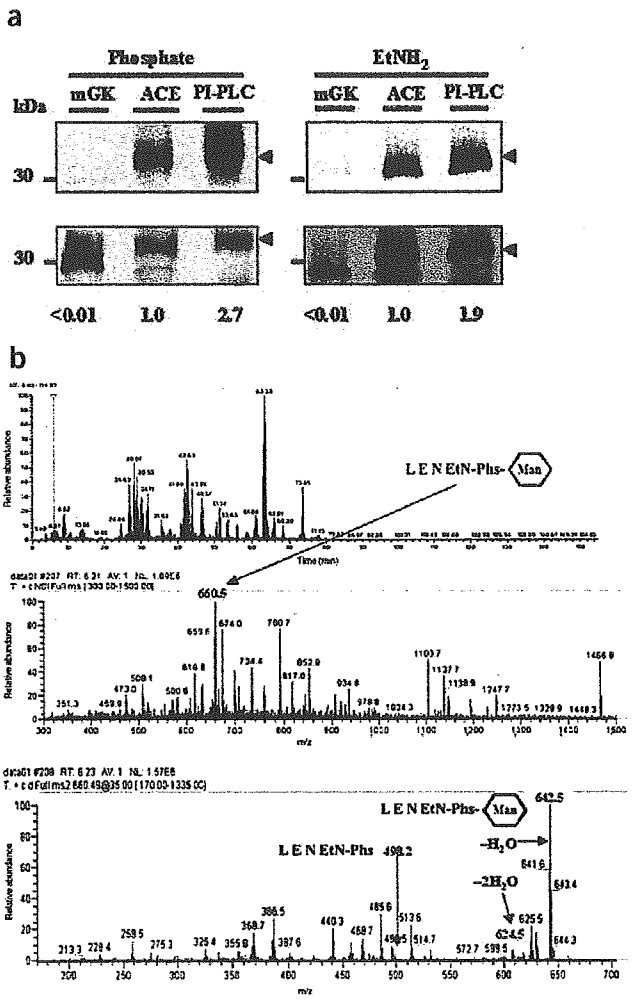

Figure 4 Characteristics of GPI cleavage by ACE. (**a**) Detection of GPI anchor moiety in the released products. Autoradiography using radioactive phosphate (top left) and ethanolamine (top right); immunoblotting of GFP (bottom panels). The radioactivity of the cognate band detected by immunoblotting (arrowhead) was determined. The radioactivity per quantity of protein is indicated (amount of ACE-treated product was considered 1.0). (**b**) Identification and characterization of carboxy-terminal peptide by high-performance liquid chromatography–mass spectrometry. Spectra of the eluted peptides are shown. The peak at the retention time (RT) of 6.2 min was considered a carboxy-terminal peptide with the indicated modification. EtN, ethanolamine; Phs, phosphate; Man, mannose. Base peak chromatogram (top). The fraction at RT = 6.2 min is indicated (red). A full-scan spectrum at RT = 6.2 min (middle). A tandem mass spectrum of m/z-660 ions (bottom).

ACE cleaved GPI anchor distal to the inositol moiety, with no influence on inositol acylation.

A recent crystallographic study has shown that positioning of Glu414 is consistent with its function and that ACE has a single fissure-like groove with zinc buried in the center[19]. Two histidines in the well-characterized core sequences of the catalytic site, HEMGH and downstream glutamate[17], are ligated with zinc. ACE-specific inhibitors also bind here, implying that this structure is indispensable for the peptidase activity. On the other hand, the results of amino acid replacements and metal chelating experiments suggest that the microstructure necessary for the GPIase activity is different from that required for peptidase activity.

High-performance liquid chromatography–mass spectrometry predicted that ACE cleaves the mannose linkage in the GPI moiety. We searched for consensus motifs of glycosidase or lectin on the ACE amino acid sequences *in silico* but found no significant similarities. Because ACE does not seem to cleave conventional sugar chain and specifically cleaves the mannose linkage of the GPI anchor, there might be some unique motifs for this activity. Serial mutagenesis of ACE could be used to determine such motifs.

Shedding of GPI-anchored proteins on the cell surface was accelerated by filipin treatment, suggesting that GPI-anchored proteins, the majority of which are packed in the lipid raft, were inherently protected from ACE attack, whereas spontaneous disruption of lipid raft was suggested on sperm capacitation, which might be caused by cholesterol depletion[38]. We believe that the sperm capacitation process includes a similar reaction caused by filipin treatment of culture cells. In this regard, GPI-anchored proteins were not released in sperms of *Ace* knockout mice (**Fig. 5a**). Considered together, our results indicate that ACE participates in the release of GPI-anchored proteins *in vivo*.

Both the peptidase-inactivated mutant of ACE and PI-PLC efficiently cured the phenotype of *Ace* knockout sperm, indicating that the release of GPI-anchored protein is crucial for the sperm binding ability. In this regard, male mice lacking angiotensinogen and kallikrein were fertile, excluding the involvement of ACE substrates such as angiotensin I and bradykinin in fertilization[39,40]. Based on these findings, our results suggest two scenarios: (i) functional activation of some GPI-anchored proteins on the sperm surface upon their release; (ii) exposure of a zona pellucida–binding factor after the shedding of some GPI-anchored proteins. By using a cell-surface biotinylation technique, we found that ACE released several proteins from the membrane fraction of germ cells (G.K., unpublished data). These proteins might also contain GPI-anchored proteins that do not directly contribute to the sperm-egg binding, although how such proteins influence sperm-egg binding remains to be investigated.

Our results also showed shedding of cell surface PrP by ACE (**Fig. 3c**). With regard to the pathogenesis of prion-related diseases, shedding of surface molecules seems to reduce the chance of pathogenic conversion[10,11]. Moreover, a soluble form of PrP also prevented the pathogenic conversion and prolonged the lifespan of scrapie-form PrP (PrP^{SC})–transferred mice[41]. Based on this scheme, we propose that ACE might be a promising compound that could prevent the production of pathogenic prion proteins. The peptidase-inactivated ACE mutant, which reduced the side effect of peptidase activity, might be potentially useful for the treatment of prion disease.

METHODS

Purification of GPI-anchored protein releasing activity. Germ cells prepared from 500 testes of adult ICR mice were crushed in a buffer containing 3 mM Tris pH 7.4, 2 mM $MgCl_2$, 1 mM EDTA, 0.25 M sucrose and Complete protease inhibitor (Boehringer Mannheim), and homogenates were centrifuged at 100,000*g*. We solubilized the pellet in a buffer containing 20 mM Tris, pH 8.0, 1% TritonX-100 and Complete protease-inhibitor. We ultracentrifuged lysates (100,000*g*), and collected the supernatant. This sample was applied to serial liquid chromatography: (i) DEAE-cellulose (Seikagaku); (ii) phenyl-Sepharose CL-4B (Amersham Bioscience); (iii) ConA-Sepharose 4B (Amersham Bioscience); and (iv) TSK gel 3000SW (Tosoh).

Mass spectrometry. To identify the 100-kDa protein, the peak fraction of TSK gel chromatogram was separated by SDS-PAGE and stained with GelCode blue stain reagent (Pierce). We excised the cognate band and digested in gel with 1.5 μg/ml trypsin (Sigma) in 50 mM ammonium bicarbonate and 5 mM $CaCl_2$ for

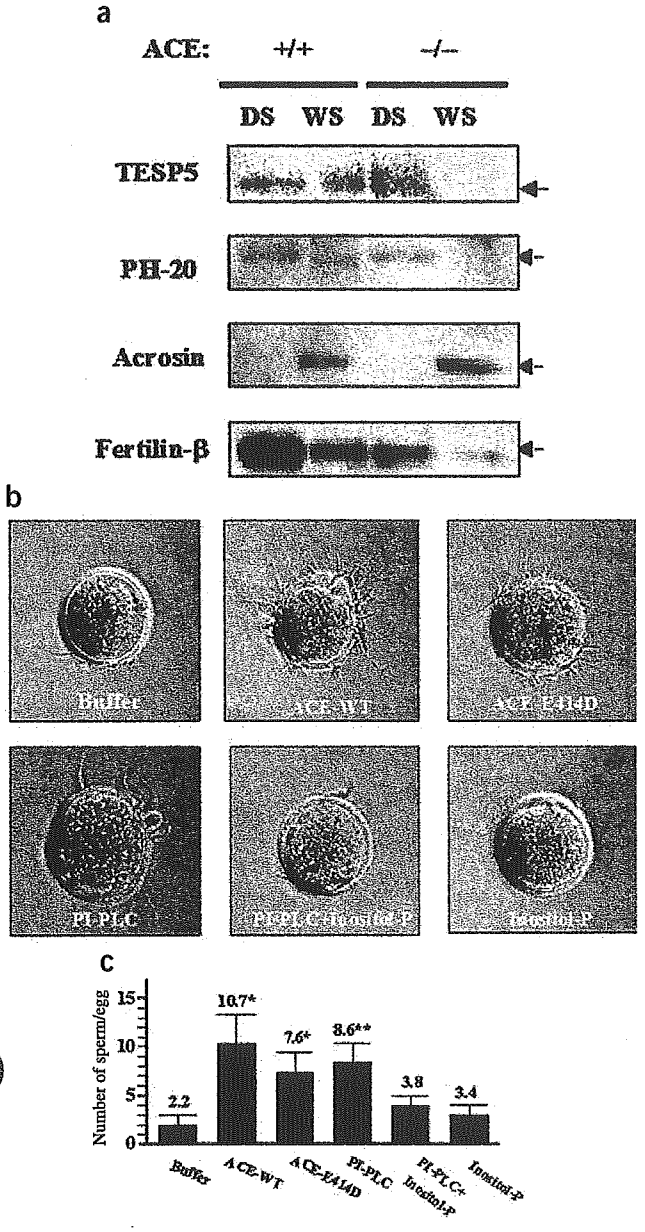

Figure 5 Involvement of ACE GPIase activity in sperm-egg binding. (**a**) Distribution of Tesp-5 (TESP5) and Ph-20 (PH-20) in the sperm of wild-type and *Ace* knockout mice detected by immunoblotting. The acrosin and fertilin-β are indicated for water-soluble and detergent-soluble fraction controls, respectively. +/+, wild-type; −/−, *Ace* knockout. DS, detergent-soluble fraction; WS, water-soluble fraction. (**b**) Binding of *Ace*-knockout sperm to the zona pellucida after various treatments. The amount of Ace used for treatment was equivalent to the endogenous ACE activity. (**c**) Number of sperm bound to the egg. Values are mean ± s.e.m. $*P < 0.001$, $**P < 0.005$, compared with buffer control; $P < 0.3$, comparison of wild-type ACE with ACE-E414D; $P < 0.5$, comparison of wild-type ACE with PI-PLC; $P < 0.05$, comparison of PI-PLC with PI-PLC + Inositol-P (Student's *t*-test).

16 h at 37 °C. After eluting peptides with 50% acetonitrile/5% formic acid several times, we applied them to the capillary high-performance liquid chromatography (Magic, Michrom)/LCQ ion-trap mass spectrometry (ThermoElectron). A perfluorinated polymer-coated electrospray tip (Fortis Tip) was used[42].The tandem mass spectra were subjected to database search using Sequest and Mascot engines. We performed two independent experiments with similar results.

We prepared the sample for investigating the structure of released EGFP-GPI as follows: we treated 1×10^9 F9 EGFP-GPI-expressing cells with 10 μg/ml filipin/phosphate-buffered saline (PBS; Sigma) for 1 h at 0 °C and then with 1.0 μM of ACE-S for 1 h at 37 °C. The released EGFP-GPI molecules were trapped with an anti-GFP antibody column, eluted with 0.1 M glycine, pH 2.8, and subjected to SDS-PAGE. We stained the gels with copper stain and destain kit (Bio-Rad) and excised the cognate band. In our experiments, the amount of released EGFP was about 30 μg. We treated all samples with trypsin and applied eluted peptides to the capillary high-performance liquid chromatography, eluted with acetonitrile gradient from 5% to 90% vol/vol and analyzed using the LCQ mass spectrometer. The tandem mass spectra were subjected to database search.

PLAP conversion assay on TritonX-114 partition. We prepared PLAP by expressing cDNA in COS7 cells, extracted it using buffer containing 20 mM Tris, pH 8.0, 150 mM NaCl, 1% TritonX-114, Complete protease inhibitor and collected the detergent-soluble phase after partitioning at 37 °C. PLAP was purified by DEAE-cellulose and anti-PLAP antibody columns. We measured PLAP activity with an alkaline phosphatase detection kit (Nacalai tesque). The conversion reaction was performed in 100 mM Tris, pH 7.5, 5 mM $CaCl_2$, 150 mM NaCl and 0.3 IU/ml of PLAP for 90 min at 37 °C. We stopped the reaction by adding TritonX-114 at a final concentration of 2% and 1 mM EDTA, followed by microcentrifugation at 25 °C. The water-soluble phase was collected and PLAP activity was measured by the alkaline phosphatase detection kit. The GPIase activity represented PLAP activity released in the water phase using the extinction coefficient of the product (32.4 $cm^{-1}mM^{-1}$) at 595 nm. To examine the metal requirement of GPIase activity, we added EDTA (Nacalai Tesque), CyDTA (Dojindo) or EGTA (Nacalai Tesque) to the assay. After stopping the reaction, we subjected the water phase to immunoblotting using a polyclonal anti-PLAP antibody (Biomeda) to detect released PLAP.

Immunoblotting. Tissue extracts were prepared as described previously[12]. The protein-transferred membranes were probed with a rabbit polyclonal antibody against GFP (Medical & Biological Laboratories), PLAP (Biomeda), TESP5 (ref. 35), PH-20 (ref. 36), acrosin or mouse monoclonal antibody against fertilin-β and detected using the ECL system (Amersham Bioscience).

ACE samples. *Ace* cDNA was obtained by reverse transcription-polymerase chain reaction (RT-PCR) using mouse testis cDNA as a template and primer pairs, 5′-TGAATTCCACCATGGGCCAAGGTTGGGCTACTCCAGG-3′ and 5′-GAATTCGTCACTTATCATCATCATCCTTATAATCCTGCTGTGGCTCCAG GTACAGGC-3′. This encodes a FLAG-tagged version of the soluble testicular isoform. Peptidase-inactivated mutants with amino acid Glu414 replaced by aspartate or His413 and His417 replaced by lysine were synthesized by site-directed mutagenesis using 5′-CTTGGTGATAGCGCACCACGATATGGGCC ACATCCAGTATTTCATGCA-3′ and 5′-CATGGAGGACTTGGTGATAGCGC ACAAGGAAATGGGCAAGATCCAGT ATTTCATGC-3′ as mutation primers, respectively. The culture supernatants of transfected COS7 cells were collected and recombinant ACE was purified by anti-FLAG M2-agarose affinity column (Sigma) and TSK gel 3000SW (Tosoh). In this study, we also used the somatic isoform of ACE (ACE-S) from rabbit lung (Sigma A-6778). The ACE peptidase activity was measured as described previously[43]. We measured both GPIase and peptidase activities of recombinant proteins and ACE-S three times independently and obtained similar results.

FACS analysis. Suspended cells were treated with 10 μg/ml filipin/PBS (Sigma) for 1 h at 0 °C. Cells (1×10^6) were then treated with 1.0 μM of ACE, 1.0 IU/ml of PI-PLC (GLYKO) or PBS alone for 1 h at 37 °C, stained with biotin-conjugated antibodies for human CD59 (ref. 44), human DAF (ref. 44), mouse Sca-1 (Pharmingen-Fujisawa), mouse Thy1.2 (Pharmingen-Fujisawa), mouse E-cadherin (Takarasyuzo) or human prion protein (3F4, Signet Laboratories), then treated with phycoerythrin-conjugated streptavidin (Pharmingen-Fujisawa) and applied to a FACScan cell sorter. EGFP-GPI expressed in F9 cells was directly detected. For quantification of shedding, we used the mean fluorescence values for each cell population to generate the percent shedding value:

$$\text{Percent shedding} = \frac{\text{ACE}(-) - \text{ACE}(+)}{\text{ACE}(-) - \text{PI-PLC}} \times 100$$

The mean fluorescence value of PI-PLC-treated population was defined as the maximum shedding and that of ACE(–) as no shedding. We performed three independent experiments and obtained similar results.

Radiolabeling analysis. We metabolically labeled F9 cells expressing EGFP-GPI with 0.2 mCi/ml of [^{32}P]-orthophosphoric acid (Amersham Bioscience) or 0.1 mCi/ml of [^{3}H]-ethanolamine (Amersham Bioscience) for 16 h. Filipin-pre-treated cells were incubated with 1.0 μM of ACE-S, 1.0 IU/ml of PI-PLC or 10% lysate of mouse submaxillary gland (containing mGK) for 1 h at 37 °C. Released EGFP was immunoprecipitated with antibody specific for GFP, subjected to SDS-PAGE and transferred onto nitrocellulose membrane. We evaluated the quantity of EGFP-GPI protein by measuring the density of bands detected on EGFP immunoblotting by using a densitometer (Molecular Device) and determined the radioactivity of the cognate band using a liquid scintillation counter (Aloka). Three independent experiments were performed with similar results.

Sperm-egg binding assay. All gametes were handled as described previously[35]. Incubated sperm (approximately 2.0×10^6 sperm/ml) were treated for 90 min with 1.0 μM wild-type Ace, 1.0 μM ACE-E414D, 1.0 IU/ml PI-PLC, or 1.0 IU/ml PI-PLC with 4 mM inositol monophosphate (Sigma), 4 mM inositol monophosphate and buffer (PBS) alone. For the sperm-egg (zona pellucida) binding assay, gametes were coincubated in a TYH droplet covered with mineral oil (Sigma) for 1 h, washed gently in PBS and fixed with 4% paraformaldehyde/PBS. The oocytes were visualized (magnification, ×200) under a light microscope (Olympus) and the number of sperm was counted at a focus showing the widest diameter of eggs. The numbers of oocytes examined were 18 in buffer only without reagents, 20 with wild-type ACE, 17 with ACE-E414D, 18 with PI-PLC, 18 with PI-PLC + inositol-P, and 17 with inositol-P alone. Three independent experiments were performed with similar results. All animal experiments were performed under approval of the Osaka University Animal Experiment Committee.

Note: Supplementary information is available on the Nature Medicine website.

ACKNOWLEDGMENTS

We thank K. Ohishi and Y. Tashima for technical assistance, T. Baba for providing anti-TESP5 antibody and P. Primakoff for providing anti-PH-20 antibody. We are also grateful to V.W. Keng and D.G. Myles for the critical reading of the manuscript. This work was supported by grants from the Osaka Medical Research Foundation for Incurable Diseases and the Ministry of Education, Science, Sports, and Culture of Japan.

COMPETING INTERESTS STATEMENT

The authors declare that they have no competing financial interests.

Received 14 May; accepted 8 December 2004
Published online at http://www.nature.com/naturemedicine/

1. Kinoshita, T., Ohishi, K. & Takeda, J. GPI-anchor synthesis in mammalian cells: genes, their products, and a deficiency. *J. Biochem.* **122**, 251–257 (1997).
2. Ikezawa, H. Glycosylphosphatidylinositol (GPI)-anchored proteins. *Biol. Pharm. Bull.* **25**, 409–417 (2002).
3. Nozaki, M. *et al.* Developmental abnormalities of glycosylphosphatidylinositol-anchor-deficient embryos revealed by Cre/loxP system. *Lab. Invest.* 79, 293–299 (1999).
4. Tarutani, M. *et al.* Tissue-specific knockout of the mouse Pig-a gene reveals important roles for GPI-anchored proteins in skin development. *Proc. Natl. Acad. Sci. USA* **94**, 7400–7405 (1997).
5. Alfieri, J. A. *et al.* Infertility in female mice with an oocyte-specific knock of GPI-anchored proteins. *J. Cell Sci.* **116**, 2149–2155 (2003).
6. Miyata, T. *et al.* The cloning of PIG-A, a component in the early step of GPI-anchor biosynthesis. *Science* **259**, 1318–1320 (1993).
7. Takeda, J. *et al.* Deficiency of the GPI anchor caused by a somatic mutation of the PIG-A gene in paroxysmal nocturnal hemoglobinuria. *Cell* **73**, 703–711 (1993).
8. Prusiner, S. B. Prions. *Proc. Natl. Acad. Sci. USA* 95, 13363–13383 (1998).
9. Aguzzi, A. & Polymenidou, M. Mammalian prion biology: one century of evolving concepts. *Cell* **116**, 313–327 (2004).
10. Marella, M., Lehmann, S., Grassi, J., & Chabry, J. Filipin prevents pathological prion protein accumulation by reducing endocytosis and inducing cellular PrP release. *J. Biol. Chem.* **277**, 25457–25464 (2002).
11. Vincent, B. *et al.* Phorbol ester-regulated cleavage of normal prion protein in HEK293 human cells and murine neurons *J. Biol. Chem.* **275**, 35612–35616 (2000).
12. Kondoh, G. *et al.* Tissue-inherent fate of GPI revealed by GPI-anchored GFP transgenesis. *FEBS Lett.* **458**, 299–303 (1999).
13. Mayor, S., Sabharanjak, S. & Maxfield, F. R. Cholesterol-dependent retention of GPI-anchored proteins in endosomes. *EMBO J.* **17**, 4626–4638 (1998).
14. Sabharanjak, S., Sharma, P., Parton, R. G. & Mayor, S. GPI-anchored proteins are delivered to recycling endosomes via a distinct cdc42-regulated, clathrin-independent pinocytic pathway. *Dev. Cell* **2**, 411–423 (2002).
15. Hooper, N. M. Angiotensin converting enzyme: implications from molecular biology for its physiological functions. *Int. J. Biochem.* **23**, 641–647 (1991).
16. Turner, A. J. & Hooper, N. M. The angiotensin-converting enzyme gene family: genomics and pharmacology. *Trends Pharmacol. Sci.* **23**, 177–183 (2002).
17. Hooper, N. M. Families of zinc metalloproteases. *FEBS Lett.* 354, 1–6 (1994).
18. Wei, L., Alhenc-Gelas, F., Corvol, P. & Clauser, E. The two homologous domains of human angiotensin I-converting enzyme are both catalytically active. *J. Biol. Chem.* **266**, 9002–9008 (1991).
19. Natesh, R., Schwager, S. L. U., Sturrock, E. D. & Acharya, K. R. Crystal structure of the human angiotensin-converting enzyme-lisinopril complex. *Nature* **421**, 551–554 (2003).
20. Crackower, M. A., *et al.* Angiotensin-converting enzyme 2 is an essential regulator of heart function. *Nature* **417**, 822–828 (2002).
21. Li, W. *et al.* Angiotensin-converting enzyme 2 is a functional receptor for the SARS coronavirus. *Nature* **426**, 450–454 (2003).
22. Scallon, B. J. *et al.* Primary structure and functional activity of a phosphatidylinositol-glycan-specific phospholipase D. *Science* **252**, 446–448 (1991).
23. Tujioka, H., Misumi, Y., Takami, N. and Ikehara, Y. Posttranslational modification of glycosylphosphatidylinositol (GPI)-specific phospholipase D and its activity in cleavage of GPI anchors. *Biochem. Biophys. Res. Commun.* **251**, 737–743 (1998).
24. Watanabe, T., Wada, N., Kim, E. E., Wyckoff, H. W. & Chou, J. Y. Mutations of a single amino acid converts germ cell alkaline phosphatase to placental alkaline phosphatase. *J. Biol. Chem.* 266, 21174–21178 (1991).
25. Carvajal, N. *et al.* Non-chelating inhibition of the H10N variant of human liver arginase by EDTA. *J. Inorg. Biochem.* **98**, 1465–1469 (2004).
26. Nyborg, J. K. & Peersen, O. B. That zincing feeling: the effect of EDTA on the behaviour of zinc-binding transcriptional regulators. *Biochem. J.* **381**, e3–e4 (2004).
27. Nicholas, B-J. *et al.* Rapid cycling of lipid raft markers between the cell surface and Golgi complex. *J. Cell Biol.* **153**, 529–541 (2001).
28. Simons, K. & Ikonen, E. Functional rafts in cell membranes. *Nature* **387**, 569–572 (1997).
29. Brown, D. A. & London, E. Functions of lipid rafts in biological membranes. *Annu. Rev. Cell Dev. Biol.* **14**, 111–136 (1998).
30. Varma, R. & Mayor, S. GPI-anchored proteins are organized in submicron domains at the cell surface. *Nature* **394**, 798–801(1998).
31. Hanada, K., Izawa, K., Nishijima, M. & Akamatsu, Y. Sphingolipid deficiency induces hypersensitivity of CD14, a glycosylphosphatidylinositol-anchored protein, to phosphatidylinositol-specific phospholipase C. *J. Biol. Chem.* **268**, 13820–13823 (1993).
32. Chen, R. *et al.* Mammalian glycosylphosphatidylinositol anchor transfer to proteins and posttransfer deacylation. *Proc. Natl. Acad. Sci. USA* **95**, 9512–9517 (1998).
33. Krege, J. H. *et al.* Male-female differences in fertility and blood pressure in ACE-deficient mice. *Nature* **375**, 146–148 (1995).
34. Hagaman, J. R., *et al.* Angiotensin-converting enzyme and male fertility. *Proc. Natl. Acad. Sci. USA* **95**, 2552–2557 (1998).
35. Honda, A., Yamagata, K., Sugiura, S., Watanabe, K. & Baba, T. A mouse serine protease TESP5 is selectively included into lipid rafts of sperm membrane presumably as a glycosylphosphatidylinositol-anchored protein. *J. Biol. Chem.* **277**, 16976–16984 (2002).
36. Lin, Y., Mahan, K., Lathrop, W. F., Myles, D. G. & Primakoff, P. A hyaluronidase activity of the sperm plasma membrane protein PH-20 enables sperm to penetrate the cumulus cell layer surrounding the egg. *J. Cell Biol.* **125**, 1157–1163 (1994).
37. Roberts, W. L., Myher, J. J., Kuksis, A., Low, M. G. & Rosenberry, T. L. Lipid analysis of the glycoinositol phospholipid membrane anchor of human erythrocyte acetylcholinesterase. Palmitoylation of inositol results in resistance to phosphatidylinositol-specific phospholipase C. *J. Biol. Chem.* **263**, 18766–18775 (1988).
38. McLeskey, S. B., Dowds, C., Carballada, R., White, R. R. & Saling, P. M. Molecules involved in mammalian sperm-egg interaction. *Int. Rev. Cytol.* **177**, 57–113 (1998).
39. Doan, T. N., Gletsu, N., Cole, J. & Bernstein, K. E. Genetic manipulation of the renin-angiotensin system. *Curr. Opin. Nephrol. Hypertens.* **10**, 483–491 (2001).
40. Bergaya, S., *et al.* Decreased flow-dependent dilation in carotid arteries of tissue kallikrein-knockout mice. *Circ. Res.* **88**, 593–599 (2001).
41. Meier, P., *et al.* Soluble dimeric prion protein binds PrP^{Sc} in vivo and antagonizes prion disease. *Cell* **113**, 49–60 (2003).
42. Tojo, H. Properties of an electrospray emitter coated with material of low surface energy. *J. Chromatogr. A* **1056**, 223–228 (2004).
43. Kasahara, Y. & Ashihara, Y. Colorimetry of angiotensin-I converting enzyme activity in serum. *Clin. Chem.* **27**, 1922–1925 (1981).
44. Kinoshita, T., Medof, M. E., Silber, R. & Nussenzweig, V. Distribution of decay-accelerating factor in the peripheral blood of normal individuals and patients with paroxysmal nocturnal hemoglobinuria. *J. Exp. Med.* **162**, 75–92 (1985).

The immunoglobulin superfamily protein Izumo is required for sperm to fuse with eggs

Naokazu Inoue[1], Masahito Ikawa[2], Ayako Isotani[1,3] & Masaru Okabe[1,2,3]

[1]*Genome Information Research Center,* [2]*Research Institute for Microbial Diseases,* [3]*Faculty of Pharmaceutical Sciences, Osaka University, Yamadaoka 3-1, Suita, Osaka 565-0871, Japan*

Representing the 60 trillion cells that build a human body, a sperm and an egg meet, recognize each other, and fuse to form a new generation of life. The factors involved in this important membrane fusion event, fertilization, have been sought for a long time[1]. Recently, CD9 on the egg membrane was found to be essential for fusion[2–4], but sperm-related fusion factors remain unknown. Here, by using a fusion-inhibiting monoclonal antibody[5] and gene cloning, we identify a mouse sperm fusion-related antigen and show that the antigen is a novel immunoglobulin superfamily protein. We have termed the gene *Izumo* and produced a gene-disrupted mouse line. *Izumo*$^{-/-}$ mice were healthy but males were sterile. They produced normal-looking sperm that bound to and penetrated the zona pellucida but were incapable of fusing with eggs. Human sperm also contain Izumo and addition of the antibody against human Izumo left the sperm unable to fuse with zona-free hamster eggs.

To identify factors involved in sperm–egg fusion, we used a monoclonal antibody, OBF13, against mouse sperm that specifically inhibits the fusion process[5]. The antigen was identified by separation of the crude extracts from mouse sperm by two-dimensional gel electrophoresis and subsequent immunoblotting with the monoclonal antibody. We termed the antigen 'Izumo' after a Japanese shrine dedicated to marriage. The identified spot was analysed by liquid chromatography tandem mass spectrometry (LC–MS/MS), and ten peptides that were 100% identical to a part of the sequence listed in the RIKEN full-length database (National Centre for Biotechnology Information (NCBI) accession number XM_133424) were found. The registered DNA sequence was confirmed by sequencing after polymerase chain reaction with reverse transcription (RT–PCR) with total RNA prepared from the testis. A human homologue was found as an unverified gene in the NCBI database (accession number BC034769). The gene encodes a novel immunoglobulin superfamily (IgSF), type I membrane protein with an extracellular immunoglobulin domain that contains one putative glycosylation site (Fig. 1a, b). Mouse Izumo was shown to be a testis (sperm)-specific 56.4-kDa antigen by western blotting with a polyclonal antibody raised against recombinant mouse Izumo (Fig. 1c). Izumo was also detectable as a 37.2-kDa protein by western blotting of human sperm with anti-human Izumo antibody (Fig. 1d). Izumo was not detectable on the surface of fresh sperm. Coinciding with the fact that mammalian sperm are incapable of fertilizing eggs when ejaculated and that fertilization occurs only after an exocytotic process called the acrosome reaction, both mouse and human Izumo became detectable on sperm surface only after the acrosome reaction (Fig. 1e, f). This would probably be

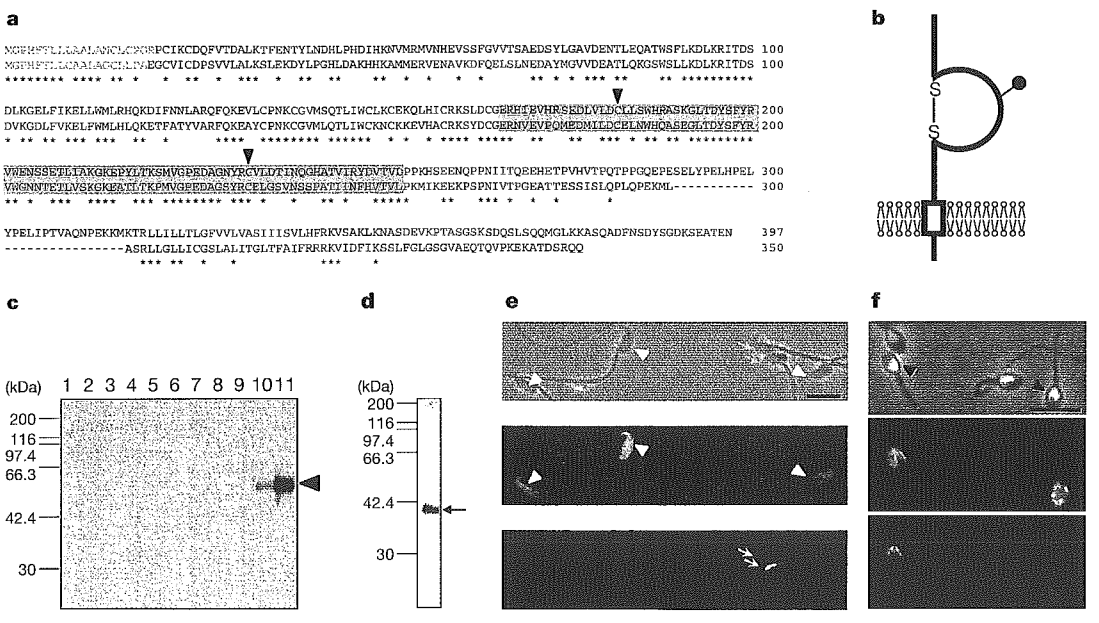

Figure 1 Identification and characterization of *Izumo*. **a**, Amino-acid sequences of mouse (upper) and human (lower) Izumo. Amino-acid identity is indicated by an asterisk. The peptide sequences obtained by LC–MS/MS are shown in red. The putative signal peptide and transmembrane region are shown in orange and blue, respectively. The immunoglobulin-like domain is boxed in green. The cysteine residues that might form a disulphide bridge are indicated by arrowheads. **b**, Izumo is a typical type I membrane glycoprotein with one immunoglobulin-like domain and a putative *N*-glycoside link motif (Asn 204). **c**, Izumo was detected exclusively in testis and sperm by western blotting. The tissues examined are, from left to right: brain, heart, thymus, spleen, lung, liver, muscle, kidney, ovary, testis and sperm. All solubilized proteins were loaded at 30 μg on each lane and detected by 1 μg ml^{-1} anti-mouse Izumo antibody. The arrowhead indicates mouse Izumo protein. **d**, Western blotting analysis of human Izumo protein from human sperm. The arrow indicates human Izumo protein. **e**, Immunostaining of Izumo in sperm from an acrosin-promoter-driven transgenic mouse line that has enhanced green fluorescent protein in the acrosome. Izumo was not detected in fresh sperm with intact acrosomes expressing EGFP[30] (indicated by green arrows), but was revealed on acrosome-reacted (non-green fluorescent) sperm (stained red, shown by white arrowheads), when stained with the polyclonal antibody against mouse Izumo. **f**, Human sperm were also stained with polyclonal anti-human Izumo antibody (red). Acrosome-reacted human sperm (stained green with anti-CD46 antibody[31]) were reactive to the antibody against human Izumo but the same antibody did not react to acrosome-intact (CD46-negative) sperm. Scale bar, 10 μm.